December 11, 2016

BACHELOR ASSIGNMENT

LOAD ESTIMATION BY WAVEFORM HARMONICS IN CLASS-E RF POWER AMPLIFIERS

R. Lohuis

Faculty of Electrical Engineering, Mathematics and Computer Science
Integrated Circuit Design

Supervisors:
dr. ir A.J. Annema
A. Ghahremani, MSc
M. Huiskamp, MSc

UNIVERSITY OF TWENTE.

Abstract

Class-E RF power amplifiers are a class of RF power amplifiers in which very high power efficiencies can be achieved. Under nominal conditions, there is no voltage across and current through the switching component at the same time. In theory, this means that there are no losses in this switching component. One big problem with these Class E power amplifiers is that these are very sensitive to load-mismatch. Because the design includes two resonant tuned tanks, small changes in load impedance can detune the circuit, resulting in load-dependent output power, power efficiency, peak voltages, peak currents and the device operating outside of safe operating area (SOA) causing degradation or failure of components. To overcome these problems a self-healing technique can be used to readjust the amplifier to the changed load impedance, by adjusting design parameters real-time. To implement this self-healing technique, the impedance of this changed load has to be known.

In this Bachelor Assignment a technique of estimating load impedances by analyzing the harmonic content of the voltage at the switching element. Lookup tables are made, noise sensitivity and accuracy are analyzed for a set of harmonics and an estimation of the performance is carried out. A single harmonic parameter does not give enough information to estimate the load accurately, so combinations of two parameters are studied.

The body diode in the FET prevents negative voltages across the capacitor and distorts the waveform. This influence is big as the estimation performance reduces drastically, making it very hard to perform load estimation when negative voltages should have appeared. A model for this behavior is made, and the load estimation technique is analyzed with this effect taken into account.

This report concludes with a performance estimation of different combinations of harmonic parameters to estimate the load impedance, presented as the estimation accuracy for each impedance plotted in a Smith chart.

Contents

1. Introduction

The class-E RF power amplifiers (Fig. 1.1) are a class of RF power amplifiers in which very high power efficiencies can be achieved. Under nominal conditions, there is no voltage across and current through the switch at the same time. These conditions are named Zero Voltage Switching (ZVS) and Zero Slope Switching (ZSS). In theory, this means that there are no losses in the switching component.

One big problem with these Class E power amplifiers is that these are very sensitive to load-mismatch. Because the design includes two resonant tuned tanks, small changes in load impedance can detune the circuit, resulting in load-dependent output power, power efficiency, peak voltages, peak currents and the device operating outside of safe operating area (SOA) causing degradation or failure of components.

To overcome these problems a self-healing technique can be used to readjust the amplifier to the changed load impedance, by adjusting design parameters real-time. To implement this self-healing technique, the impedance of this changed load has to be known.

In this Bachelor Assignment a practical way to measure this antenna impedance will be examined. The proposed method tries to combine the work of A. Ghahremani [4] and M. Huiskamp [6].

A. Ghahremani showed a load-pull analysis for class-E RF power amplifiers in [4]. In his paper, the effects of load-mismatch on the behavior of amplifiers is described. Due to load-mismatch the ZVS and ZSS conditions are violated, resulting in a nonzero voltage and slope at the switching moment. The voltage at the switching moment is referred to as the α parameter, the slope as the β parameter, as shown in Fig. 1.2. When the α and β parameters of the PA are known, all of the performance parameters are known, including antenna impedance.

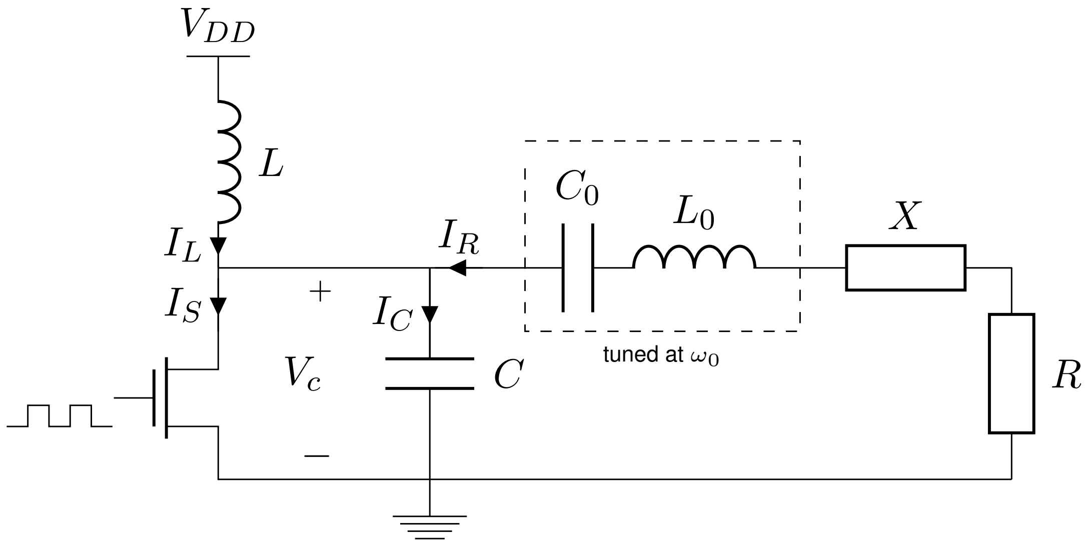

Figure 1.1: Basic Class-E RF amplifier schematic. The switch is operated by a frequency ω and the LC-tank is tuned at a frequency ω_0. R is the real load impedance, X the imaginary load impedance.

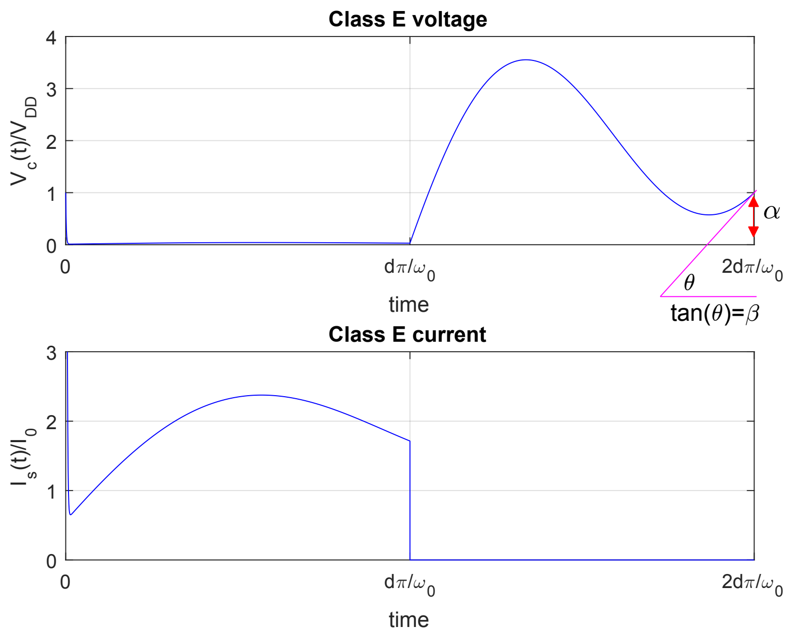

Figure 1.2: Example switch voltage of a Class E RF PA. Parameters α (Voltage across switch when switch is closing) and β (Derivative of voltage across switch when switch is closing) of a Class E RF PA are graphically shown.

The problem is that it is not easy to measure α and β directly at the switch node of the PA. The frequency of the signal is in the RF range. To measure the value of α, the voltage of the node has to be measured just before the switch closes, at $d\pi/\omega_0$ in a switching cycle. Measuring β is harder, as the slope of the voltage just before switching has to be measured, which needs very accurate ADCs.

M. Huiskamp described a system to measure and compute the harmonic content of the waveform generated at the switch node of a class-E amplifier in [6]. Using a DFT, the first three harmonics of the signal are calculated.

The goal of this Bachelor Assignment is to investigate if it is possible to use information of the harmonics of the signal at the switch node in a class-E RF PA to determine the load impedance, and how this can be done most efficiëntly. If this information is not sufficient, extra required parameters that are needed in order to determine the load impedance will be investigated.

2. Self-healing

2.1 Impedance mismatch

Load variations in Class-E RF amplifiers cause the amplifier to violate its ZVS and ZSS conditions, which means that $\alpha \neq 0$ and $\beta \neq 0$. This can result in the amplifier to operate outside the safe operating area, causing its components to fail. [1]

When the load impedance is known, the q and d parameters can be tuned such that the amplifier is 'healed' and operates within its safe operating area (SOA) again, as described in [8].

2.2 Load impedances

As stated in [4], load impedances can be defined as normalized impedances, referenced to the nominal load impedance Z_{nom}. An impedance can be expressed as

$$Z = R + jX \tag{2.1}$$

and every load impedance Z can now be expressed relatively to Z_{nom} by the scaling factors k and k' as:

$$Z = kR_{nom} + j\left(X_{nom} + k'R_{nom}\right) \tag{2.2}$$

This means, that for nominal conditions $k = 1$ and $k' = 0$. By observing the K-design set, R and X can be found in K_L and K_X[3]:

$$K_L = \frac{L\omega_0}{R} \tag{2.3}$$

$$K_X = \frac{X}{R} \tag{2.4}$$

By knowing the design set for a certain load impedance as if it was a nominal load and the design set of the actual nominal load, k and k' can be calculated as as:

$$k = \frac{K_{L,nom}}{K_L} \tag{2.5}$$

$$k' = K_X \cdot k - K_{X,nom} \tag{2.6}$$

The K-design set parameters K_L and K_X can be expressed solely by (q, d, m, α and β) [2]. For a design with fixed q, d and m, the load impedance can thus be calculated by measuring only α and β.

q	m	d	α	β
1.412	0.05	1	0	0

Table 2.1: Simulation parameters used for the Class-E simulations in *matlab*. These are conventional design numbers for high output power and high efficiency. [4]

α and β are defined by V_C, the voltage of the capacitor:

$$\alpha = \frac{V_c\left(\frac{2\pi}{\omega_0}\right)}{V_{DD}} \tag{2.7}$$

$$\beta = \frac{\frac{dV_c}{dt}\left(\frac{2\pi}{\omega_0}\right)}{V_{DD}\omega_0} \tag{2.8}$$

This means that α is defined as the relative voltage at the end of a cycle, and β is defined as the slope of the relative voltage, relative to the operating frequency, at the end of a cycle as graphically shown in Fig. 1.2.

The other way around, the design set can also be calculated for every load impedance using only variable α and β parameters. Using the design set, the capacitor voltage V_C can be calculated. By applying a Fast Fourier Transform, it is easy to calculate the harmonic contents.

A *matlab* script it used to simulate a class-E RF amplifier, by calculating the K-design set, V_C and I_S for a given set (q, d, m) and α and β, as shown in Table 2.1. α and β can be swept over a certain range of values to calculate the amplifier for multiple operating points. By using (2.2), (2.5) and (2.6), the load impedances of these variable α and β simulations can calculated relatively to a nominal operation point where $\alpha = 0$ and $\beta = 0$. To describe different load impedances in a convenient way, reflection coefficients and Smith Charts normalized to the nominal load impedance are used. The reflection coefficient Γ_Z is defined as [7]:

$$\Gamma_Z = \frac{Z - Z_{nom}}{Z + Z_{nom}} \tag{2.9}$$

For simplicity, in numerical calculations a nominal impedance of $R_{nom} = 1\,\Omega$ and $X_{nom} = 0\,\Omega$ ($Z_{nom} = 1\,\Omega$) is used.

The simulation results provide relations between α, β, k, k' and harmonic content. As Eq. (2.2) states a direct relation between relative impedance and k and k', there is a relation between the harmonic content and the relative impedance. As the harmonic content can be measured [6] quite good, an impedance estimation should also be possible if as set of harmonic parameters is unique enough for every possible impedance.

2.3 Lookup table

By building loop-up tables with harmonic parameters and relative impedances, an unknown load impedance can be estimated by measuring the harmonic parameters of

V_C, looking up these parameters in the table and finding the corresponding k and k' to calculate the impedance. To create such look-up tables, the following steps are taken:

1. Calculate a table of alpha and beta parameter values, so that the corresponding load impedances fill the entire Γ_Z-plane.
2. Simulate all α and β combinations in this table, calculate waveforms and impedances.
3. Calculate the harmonic parameters by performing a FFT for the acquired waveforms for all entries in the table.
4. Resample the harmonic parameters to create look-up tables that are evenly spaced on the Γ_Z-plane.

These steps are explained in the next chapter. To estimate the performance of the use of these lookup tables several tests and comparisons are shown in the following chapters.

3. Harmonics look-up table

3.1 Look-up table calculation

First, a table of alpha and beta values is generated, so the entire Smith Chart is covered. A *matlab* script based on the expressions for the switch-node voltage, the switch current and the K-design set, a plot of the α and β values is calculated and shown in a Smith Chart in Fig. 3.1. The figure shows that alpha values between ~ -8.5 and ~ 8.5 results in a nonnegative loads. For beta, values between $sim - 2$ and ~ 30 covers the Smith chart. The alpha parameter shows an almost linear distribution along the chart. Therefore the table of alpha values is chosen to be linear as well. The beta parameter shows a more logarithmic relation between the value and the Smith Chart. By heuristic optimization, a set $b[n] = b[n-1] + b[1]$ with $b[1] = -2$ is found to show a near linear scale on the Smith Chart. To optimize simulation times, the step size is varied for different simulations so that for simple simulations a table of $\sim 300\times \sim 300$ values can be used and for final results a table of $\sim 2000\times \sim 2000$ values can be used to increase the resolution.

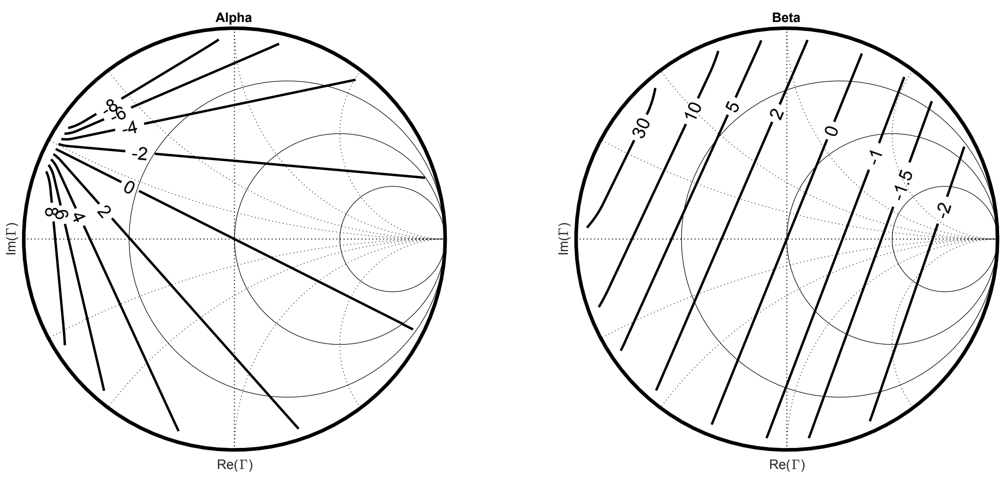

(a) Plot of α-parameter.

(b) Plot of β-parameter.

Figure 3.1: Constant α and β contours in the $\Gamma_{Z'}$ plane.

A lot of the combinations of an alpha and beta parameter fall outside the unit circle of the reflection coefficient C on the Smith Chart, meaning the the waveform would have been produced by a negative load. Because these results are not relevant, these points are filtered out later on by testing if the absolute value of the reflection coefficient Γ_Z is not greater than 1.

3.2 Simulation and FFT

After creating a table with alpha and beta values, the *matlab* simulation script is used to simulate the Class-E amplifier for all these alpha and beta values. For each entry, the current and voltage waveforms and the design sets are calculated. By comparing the K_L and K_X parameters to the values of the reference impedance $\Gamma_{Z,nom} = 0$, the scaling factor k and k' can be extracted. The load impedance scales with the same factors, as explained in Eq. (2.2), so now also the impedance of each point can be calculated.

A Fast Fourier Transformation (FFT) is used to calculate the amplitude and phase of the harmonics. The results of the first six harmonics and DC are stored for each table entry. Because a FFT gives two results: a real part and an imaginary part, or an amplitude and a phase, each each now gives 6 harmonics with 4 parameters per harmonic. As DC has gives no phase information (which means that its imaginary part is zero, the phase is zero and the absolute value is equal to the real value) this means that every point in the grid now has 25 parameters that can be used to estimate an impedance. The naming of these parameters used in this report is shown in Table 3.1.

Table 3.1: All 25 harmonic parameters used in this assignment.

	$\lvert h_n \rvert$	$\angle h_n$	$\mathrm{Re}\, h_n$	$\mathrm{Im}\, h_n$
0th	-	-	h_{0r}	-
1st	h_{1a}	h_{1p}	h_{1r}	h_{1i}
2nd	h_{2a}	h_{2p}	h_{2r}	h_{2i}
3rd	h_{3a}	h_{3p}	h_{3r}	h_{3i}
4th	h_{4a}	h_{4p}	h_{4r}	h_{4i}
5th	h_{5a}	h_{5p}	h_{5r}	h_{5i}
6th	h_{6a}	h_{6p}	h_{6r}	h_{6i}

3.3 Resampling of the table

Because the data points on the Smith Chart are not equally spread, it is more difficult to perform calculations on the dataset. Therefore, all arrays are resampled to an equally spaced grid. This is done within *matlab* with the use of linear interpolation. The result of this operation is a set of look-up tables, that contain information about the first six harmonics and DC, for the reflection coefficient $|\Gamma_Z| < 1$.

Now the harmonic data is stored in an equally spaced grid, the data can be plot easily by *matlab*. Smith Charts containing the information of all 25 parameters are shown in Figs. A.1 to A.5 in Appendix A.

4. Performance

4.1 Gradient

In order to determine which of the parameters give the most and most accurate information for determining the load impedance, the rate of change of the values is important. A bigger change in a value gives a higher accuracy. To find how big these differences are and in which direction the biggest differences are found, the gradients $\nabla h_n\left(\mathit{\Gamma}_Z\right)$ are calculated for all 25 fields. The mean values of the amplitude of the gradients are shown in Table 4.1. These values shown the mean difference in the strength of the harmonic parameter for a reflection coefficient change of 1. This table shows that the 0th harmonic (DC) gives littlest information of all harmonics, as the amplitude changes least compared to the other harmonics for all loads plotted on the $\mathit{\Gamma}_Z$ plane. Also, the first and second harmonic have the strongest gradients, while the amplitude is decreasing with the order of the harmonic.

The gradients of the absolute value, phase, real part and imaginary part of the first six harmonics and DC (only real part) are shown in Figs. B.1 to B.5 in Appendix B. In these figures it can be seen that the amplitude of the gradient is largest in the upper left region ($\mathrm{Re}(\mathit{\Gamma}_Z) > 0, \mathrm{Im}(\mathit{\Gamma}_Z) < 0$) for most parameters. Therefore, the largest accuracy for finding impedances will be found in this region as well.

The direction of the gradients is also very important as it indicates in which direction the harmonic changes the most. To estimate a load given its harmonics, at least two harmonics are needed to find an unique spot on the two dimensional, complex $\mathit{\Gamma}_Z$ plane. The more orthogonal these harmonics are distributed over this plane, the more accurate this look-up table for finding impedances is.

Table 4.1: Mean gradient amplitude for different complex harmonic content variables in $\frac{1}{1 \times 10^3}$ $(\frac{1}{\Gamma_Z})$

	Amplitude	**Phase**	**Re**	**Im**
0th	-	-	0.9393	-
1st	146.8941	0.1196	196.7789	38.0400
2nd	200.0732	0.5047	86.6997	201.9473
3rd	90.1820	0.1892	73.7422	59.8290
4th	36.0454	0.6067	10.5596	40.1343
5th	35.1720	0.1857	22.3227	30.3400
6th	22.3516	0.6149	4.6608	24.5324

4.2 Noise sensitivity

To calculate a form of noise sensitivity per harmonic parameter, mean noise contribution N_{h_n} to all harmonic parameters is calculated. This is done by simulation the circuit again for different α and β values. First the waveform is calculated and copied a thousand times. At every copy, White Gaussian Noise (WGN) with a peak-to-peak voltage of $1\frac{V}{V_{dd\,pp}}$ is added and the harmonics are calculated using a FFT. Then, these values are compared to the noiseless simulation and the average value of all copies is calculated. This value now represents how sensitive the harmonic parameters are to fluctuations in the signal V_C, described as harmonic amplitude per $\frac{V}{V_{dd\,pp}}$ noise. In Table 4.2 the sensitivity values are shown.

The gradients (in harmonic amplitude per $\Delta\Gamma_Z$) can be combined with the noise sensitivity of the harmonic parameters (in harmonic amplitude per noise amplitude), to calculate how much deviation in reflection coefficient Γ_Z in the optimal direction (gradient) will occur, when $1\frac{V}{V_{dd\,pp}}$ AWGN is added to the waveform of V_C. This error sensitivity ϵ_{Γ_Z} is calculated as:

$$\epsilon_{\Gamma_Z,mean} = \frac{N_{h_n}}{|\nabla h_n|_{mean}} \tag{4.1}$$

These values are shown in Table 4.3. For the load estimation process multiple harmonic parameters are used. Because of this, the direction of the gradient is the most important for noise, as other directions are corrected by other harmonic parameters.

Table 4.2: Noise sensitivity of harmonics: Mean difference in harmonic parameters for 1 $\frac{V}{V_{dd\,pp}}$ Additive White Gaussian Noise.

	Amplitude	Phase	Re	Im
0th	-	-	10.2886	-
1st	7.2770	0.0056	7.2782	7.2740
2nd	7.2756	0.0148	7.2764	7.2773
3rd	7.2782	0.0150	7.2778	7.2776
4th	7.2784	0.0794	7.2771	7.2764
5th	7.2739	0.0382	7.2776	7.2786
6th	7.2613	0.1337	7.2779	7.2776

Table 4.3: Mean noise error in in 1×10^{-3} $(\mathit{\Gamma}_Z)$, optimal direction for 1 $\frac{V}{V_{dd\,pp}}$ Additive White Gaussian Noise. The numbers represent the mean deviation in reflection factor for AWGN: a lower number means that the parameter is less sensitive for noise on V_C.

	Amplitude	Phase	Re	Im
0th	-	-	10.9535	-
1st	0.0495	0.0465	0.0370	0.1912
2nd	0.0364	0.0294	0.0839	0.0360
3rd	0.0807	0.0795	0.0987	0.1216
4th	0.2018	0.1309	0.6891	0.1813
5th	0.2068	0.2056	0.3260	0.2399
6th	0.3249	0.2174	1.5615	0.2967

4.3 Combinations

As can be seen in the contour plots and gradients of the harmonic parameters, one parameter does not provide enough information for accurate load estimation, as high accuracy is only provided in one direction, the direction of the gradient. When combining two parameters and using both look-up tables, the accuracy can be extended to two directions. The more perpendicular those directions are, the more accurate the load on the two-dimensional $\mathit{\Gamma}_Z$ plane can be estimated. When the directions of the gradients are parallel, more accuracy in that direction is given, but accuracy in all other directions is still too bad for load estimation.

To provide a measure of information of two parameters, a *combined sensitivity value* $C_{nm}\left(\mathit{\Gamma}_Z\right)$, as function of the reflection coefficient $\mathit{\Gamma}_Z$, is introduced. The number represents the accuracy of using the two corresponding look-up tables to estimate an impedance. The higher the gradients, the more accurate the look-up tables are. By comparing the angles of the two gradients, the degree of perpendicularity can be calculated. The value is defined as the product of the length of the gradients, multiplied with the sine function of the angle difference and divided by the noise sensitivity:

$$C_{nm}\left(\mathit{\Gamma}_Z\right) = \frac{\left|\nabla h_n\left(\mathit{\Gamma}_Z\right)\right|}{N_{h_n}} \cdot \frac{\left|\nabla h_m\left(\mathit{\Gamma}_Z\right)\right|}{N_{h_m}} \cdot \sin\left(\left|\angle h_n\left(\mathit{\Gamma}_Z\right) - \angle h_m\left(\mathit{\Gamma}_Z\right)\right|\right) \tag{4.2}$$

The sine function makes sure that perpendicular gradients cancel, resulting in a information grade of zero, and orthogonal gradients result in just the multiplication of the gradient amplitudes. A higher noise sensitivity (Table 4.2) results in a lower sensitivity value.

By combining the 25 different parameters, $\sum\limits_{k=1}^{25-1} k = \frac{(25-1)\cdot 25}{2} = 300$ combinations can be made. All resulting values are calculated for each point in the $\mathit{\Gamma}_Z$ plane. For comparison, the mean sensitivity value for the combinations is calculated and shown in Table 4.4. A graphical representation is shown in Fig. 4.1. The results show that combinations with the 0th harmonic (DC) has a significantly lower sensitivity value than the combinations with other harmonics. This has to do with the small differences in DC amplitude. The results also show that combinations with the 1st, 2nd and 3rd harmonics (the upper left corner of Fig. 4.1) gives the most information, as the gradients have high amplitudes. The best 6 combinations are shown in Table 4.4 as numerical mean values and graphically for the entire $\mathit{\Gamma}_Z$-plane in Fig. 4.2, as these values stand out compared to the other values.

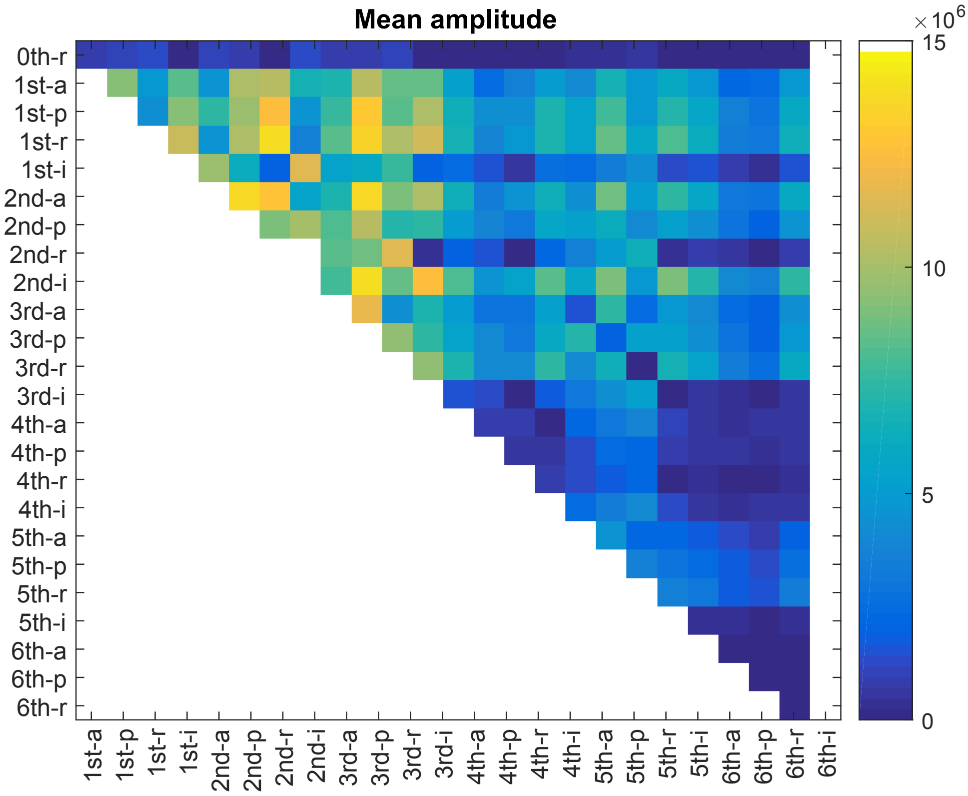

Figure 4.1: Color plot with the sensitivity values of all combinations. A higher value means more accuracy for load impedance estimation. A table with all numerical values can be found in Table C.1 in Appendix C.

Table 4.4: Mean sensitivity value $C_{nm} \times 10^7$ for different combinations of harmonics. This table is a subset of the complete Table C.1 in Appendix C. The combination with the six largest values are shown in gray.

	h_{1r}	h_{2a}	h_{2i}	h_{3p}
h_{2p}	1.01	1.37	1.01	1.04
h_{2r}	1.39	3.47	1.55	0.89
h_{2i}	0.36	3.22	-	1.40
h_{3p}	1.36	1.38	1.40	-

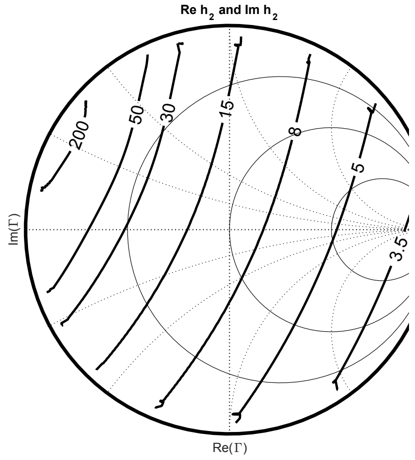

h_{2r} and h_{2i}

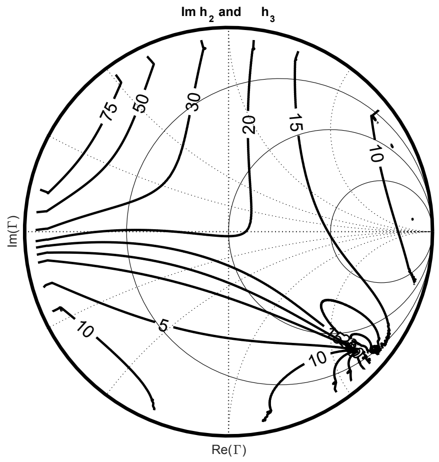

h_{2i} and h_{3p}

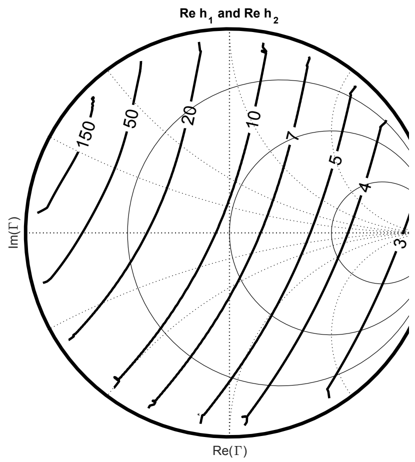

h_{1r} and h_{2r}

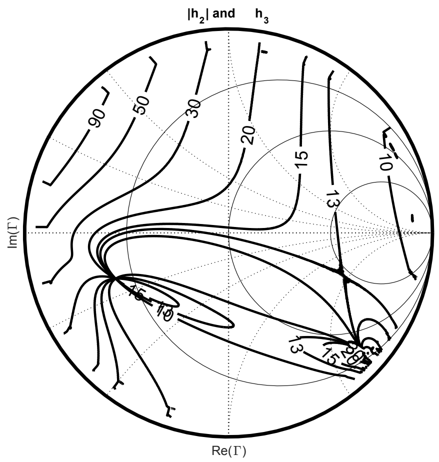

h_{2a} and h_{3p}

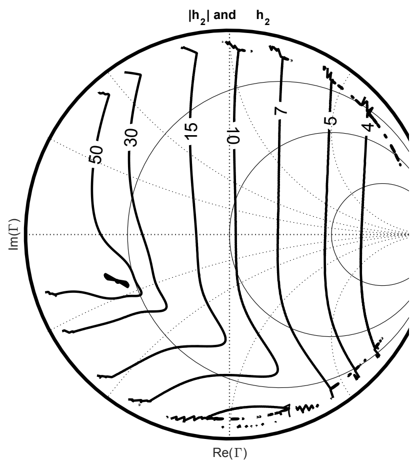

h_{2a} and h_{2p}

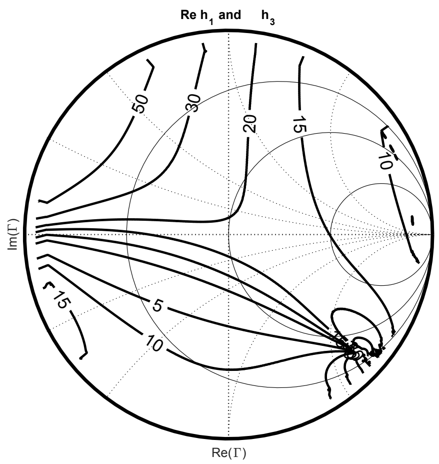

h_{1r} and h_{3p}

Figure 4.2: Combined sensitivity graph, showing the combined sensitivity values for the entire Γ_Z-plane, for the 6 combinations with the highest average combined sensitivity value.

4.4 Error calculation

Because for load estimation the measured harmonic parameters has a certain error, it is important to known how much this influences the result of the estimation. To indicate the accuracy of a combination, the maximum difference in estimated reflection coefficient can be calculated for a given parameter offset.

Because this *error sensitivity* is dependent of the load, this sensitivity can be calculated for the entire $\mathit{\Gamma}_Z$-plane.

The calculations are done by finding the maximum difference between $\mathit{\Gamma}_Z$ for a given reflection coefficient, and all reflection coefficients that have harmonic parameters in a given range of the parameters for the original reflection coefficient. The range is defined by the noise sensitivities in Table 4.2. The error now defines the maximum error in the estimated $\mathit{\Gamma}_Z$ when V_C with AWGN 1$\frac{V}{V_{dd\,pp}}$ distortion is measured for each point on the $\mathit{\Gamma}_Z$-plane, given the combinations of harmonic parameters used for the estimation.

The error is calculated for the six combinations with the highest mean combined sensitivity values found in Table 4.4. The results are shown in Fig. 4.3.

The results show that these results are in accordance with the combined sensitivity values shown in Fig. 4.2, as lower sensitivity leads to more $\mathit{\Gamma}_Z$-error. As different combinations lead to different optimal $\mathit{\Gamma}_Z$ areas where the $\mathit{\Gamma}_Z$-error is low, combinations of more than two harmonic parameters should lead to even more optimal solutions.

For the first combination, consisting of h_{2r} and h_{2i}, the maximum error is $\mathit{\Delta\Gamma}_Z = 0.1$

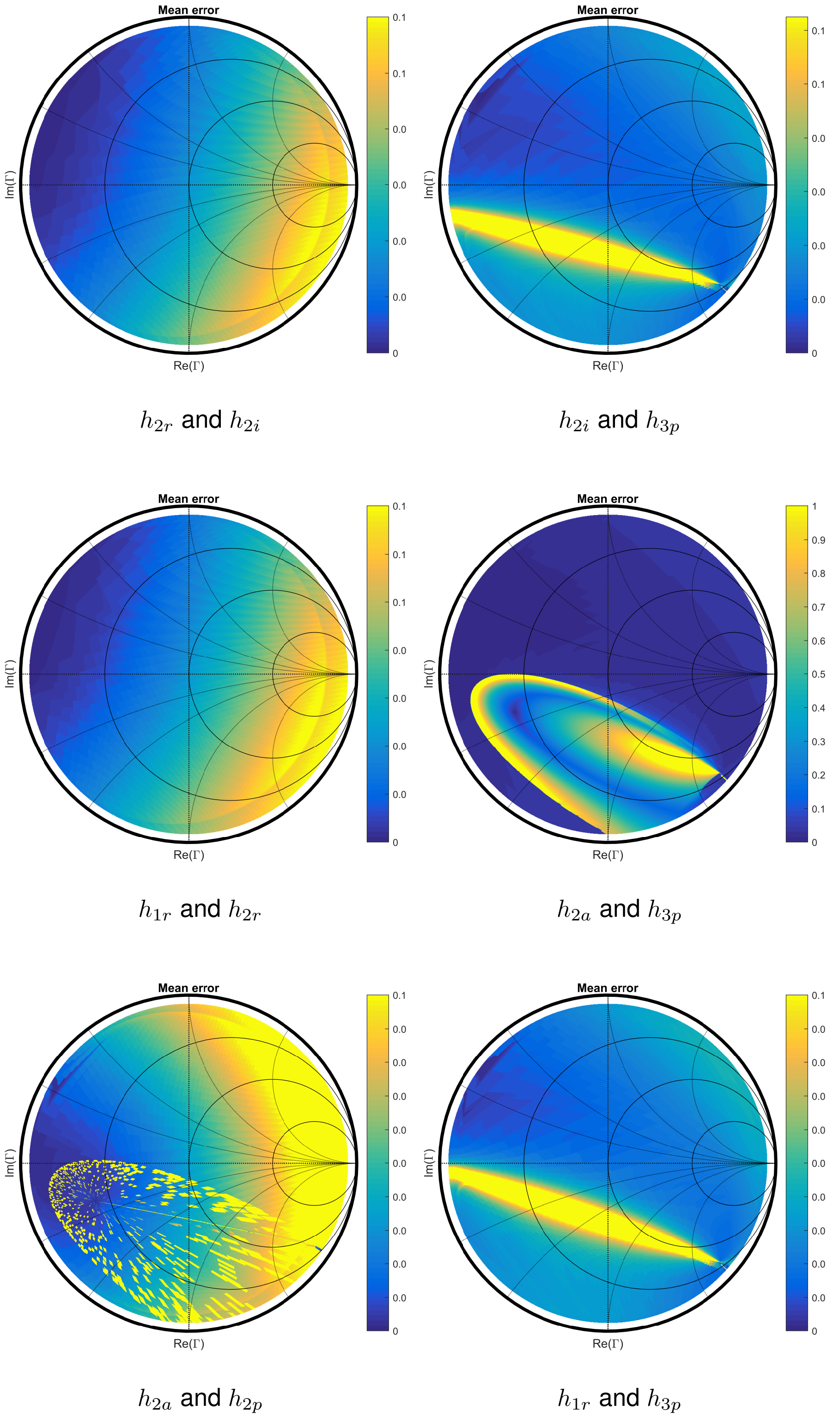

Figure 4.3: Maximum $\varGamma_Z$ error for an offset in harmonic parameters caused by AWGN 1 $\frac{V}{V_{dd\,pp}}$ distortion, when estimation $\varGamma_Z$ by use of different combinations of harmonic parameters.

4.5 Testbench

To test the actual performance of this estimation technique, a testbench is made. This testbench can create waveforms for a given set of design parameters, including the α and β parameters, and creates copies of this waveform with *Additive White Gaussian Noise* (AWGN) with a peak-to-peak voltage of $1\frac{V}{V_{dd}}$. For all of these waveforms the harmonics are calculated. The testbench can be adjusted to use a given set of harmonic fields (amplitude, phase, real part and imaginary part for every harmonic) and tries to find the closest estimation for the waveforms on the calculated look-up fields. The closest estimation, which is defined as the table entry with the lowest value of the summation of errors between the value of the tested waveform and the look-up table for each field, determines the estimated load impedance. All impedances are plotted on a Smith Chart and the mean distance between the estimated reflection coefficient and the estimated reflection coefficient of the original undistorted waveform is calculated. This gives an estimation about how accurate the load can be estimated given a noise power for distortion of the to be estimated simulated waveform.

In Fig. 4.4, testbench results of single harmonic parameters are shown. These harmonics are most used in the six combinations with the highest mean combined sensitivity values. The first plot shows a noise signal used in the testbench. In Fig. 4.4a, the undistorted voltage waveform is shown in blue, and one instantiation of the voltage distorted with White Gaussian Noise is shown in red. In Figs. 4.4b to 4.4f, the estimated load impedances are plotted on a Smith Chart. Each point is estimated by the the same voltage waveform but has a different instantiations of White Gaussian Noise. Lines become visible and show that using the given harmonic parameter for estimation, (small) disturbances in the voltage measurement can result in estimated impedances somewhere on these lines.

The shapes are in accordance with the contour plots shown in Figs. A.1 to A.5 in Appendix A: The gradients show the directions of the largest changes in parameters, and thus the most sensitive direction. These testbench results shown that indeed disturbances on the measured signal result in estimated impedances distributed over the contour line that touches the point in Γ_Z that corresponds to the simulated impedance, which is Z_{nom}.

When multiple parameters are combined to estimate the load impedance, load impedances are only found in the area where the corresponding lines of the parameters overlap, thus increasing the accuracy of the estimation.

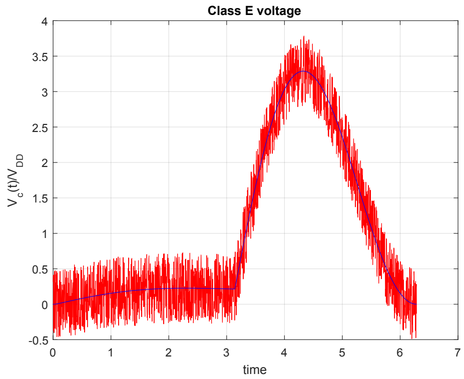

(a) Simulated V_C for $\alpha = 0$ and $\beta = 0$. black the original signal, in red the add White Gaussian Noise.

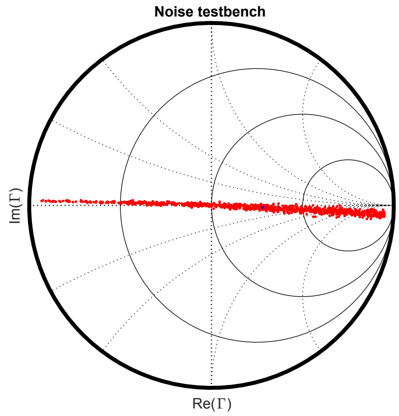

(b) h_{2r}

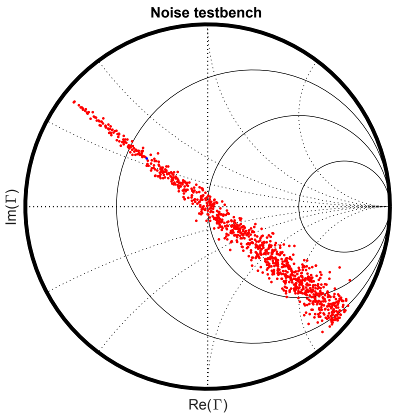

(c) h_{3i}

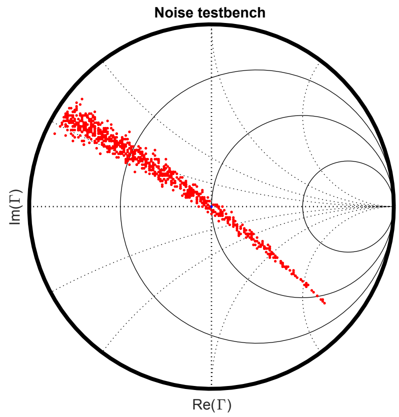

(d) h_{3p}

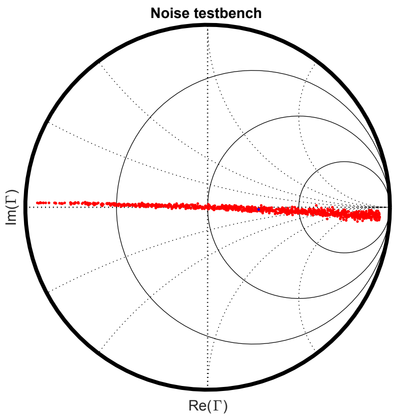

(e) h_{1r}

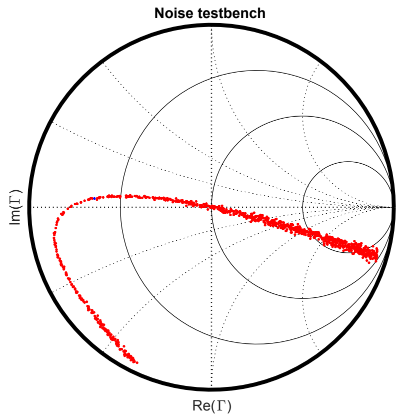

(f) h_{2a}

Figure 4.4: Estimated load impedance by using specified harmonic parameters for $\alpha = 0$ and $\beta = 0$ with AWGN 1 $\frac{V}{V_{dd\,pp}}$ distortion.

The testbench results of the six combinations found in Table 4.4 are shown in Fig. 4.5 for $\alpha = 0, \beta = 0$. The testbench shows that the combination of h_{2r} and h_{2i} gives the lowest mean error, as predicted with the error estimation. The combined sensitivity value, is an indication for the entire $\mathit{\Gamma}_Z$-plane, and not just for the simulated $\alpha = 0, \beta = 0$. This explains why the h_{2a} and h_{3p} combination performs worse, and the h_{2a} and h_{2p} combination performs much better than expected from the sensitivity value. The combined sensitivity values therefore give a more general approximation of the performance of a combination, while the testbench can show exact results at a given $\mathit{\Gamma}_Z$.

As the h_{2r} and h_{2i} combinations gives the best result in numerical gradient comparison and in the testbench, this set of parameters is used to test different values for α and β. The results are shown in Fig. 4.6. As expected from the amplitude of the gradients (Figs. B.1 to B.5 in Appendix B) and combination (Fig. 4.2), most accuracy is found in the upper left corner of the Smith Chart, where $\mathrm{Re}\,\mathit{\Gamma}_Z < 0$ and $\mathrm{Im}\,\mathit{\Gamma}_Z > 0$. This area represents an inductive load with a real impedance higher than the nominal impedance.[5] Lower impedances than the nominal impedance and more capacitive loads leads to more error in the estimation.

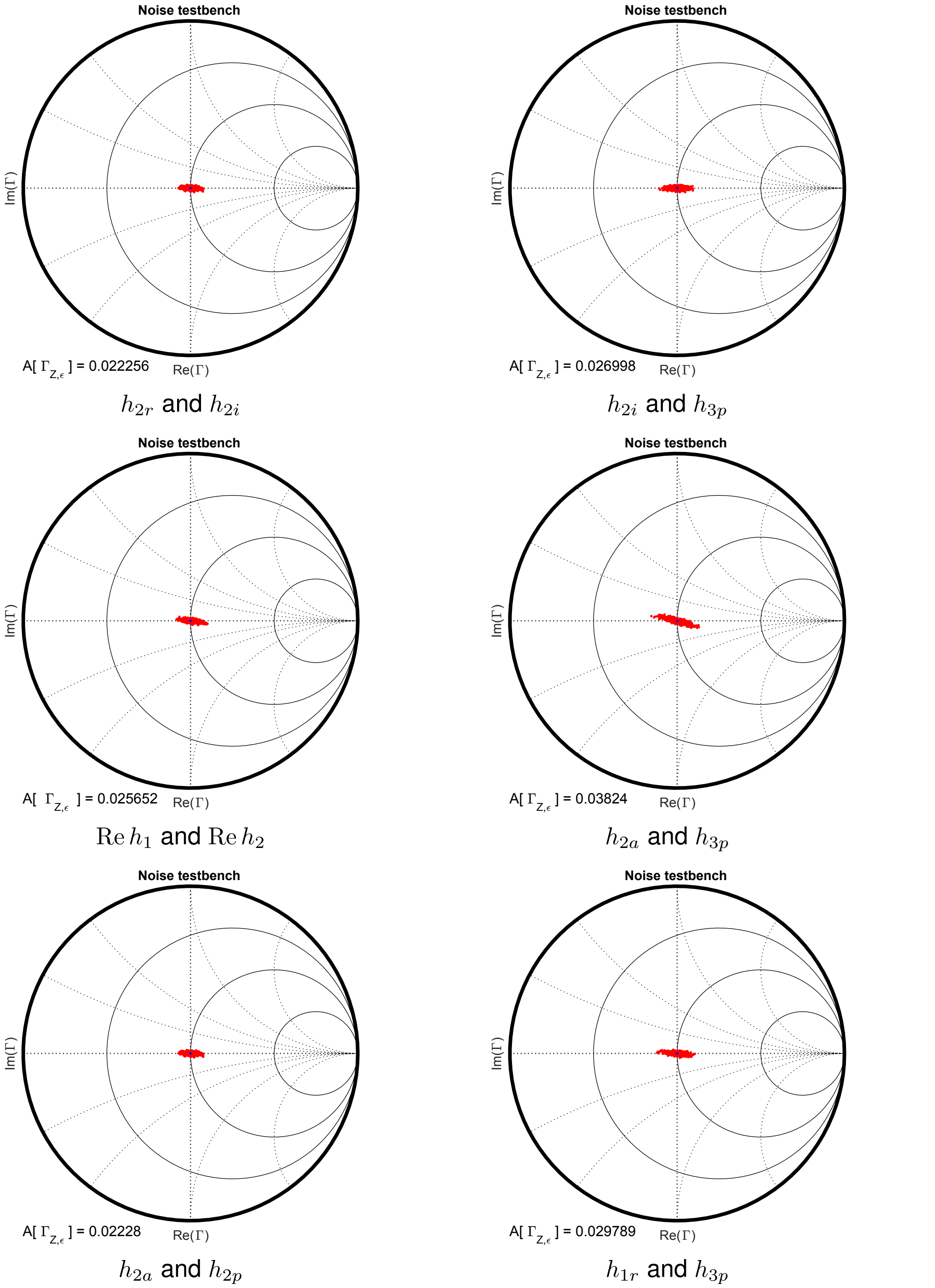

Figure 4.5: Performance of the load estimation by AWGN 1 $\frac{V}{V_{dd\,pp}}$ distortion for $\alpha = 0$ and $\beta = 0$ and a combination of two harmonic parameters. Different combinations of harmonic parameters for load estimation are shown. For each combination the mean error A $[\Gamma_{Z,\epsilon}]$ is specified.

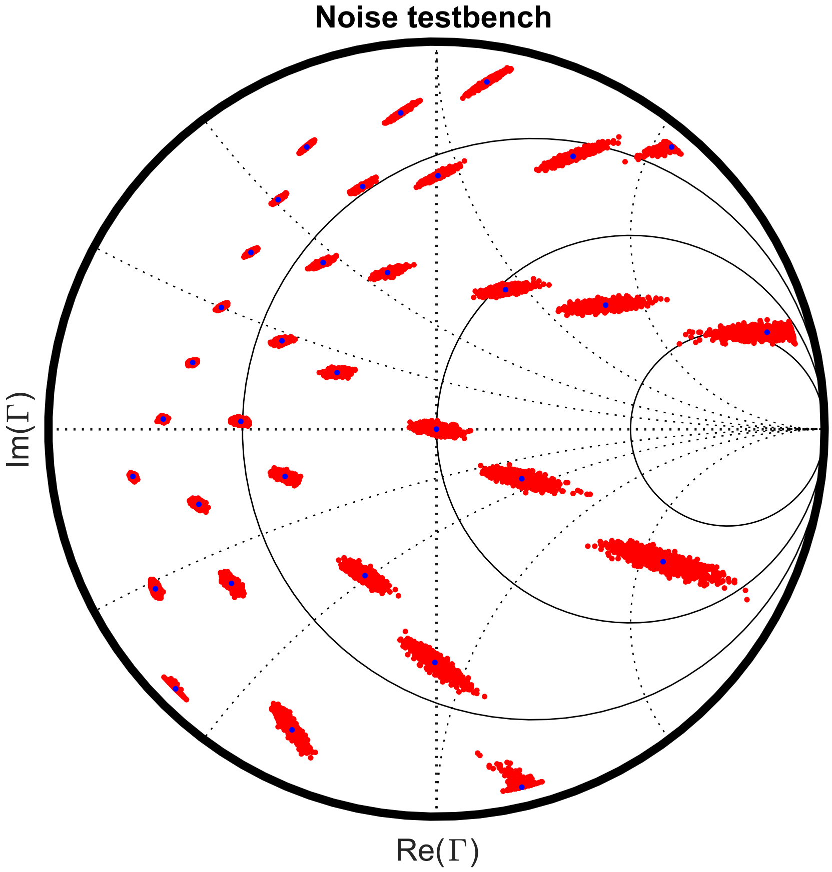

Figure 4.6: Noise testbench results for multiple values of α and β ($\alpha = \{-6, -4, -2, 0, 2, 4, 6\}$, $\beta = \{-2, -1, 0, 2, 4, 8\}$). The blue dot represents the actual load impedance. Red dots represent load impedance estimations estimated from copies with AWGN($1\frac{V}{V_{dd}}$) added to the voltage.

5. Diode

5.1 FET body diode

In the *matlab* simulation, there is one physical aspect of the Class-E circuit that is ignored, that has an enormous impact on the waveform of V_C, namely that a FET is not an ideal switch and has a body diode. This diode is shown in Fig. 5.1. When the voltage over the capacitor becomes negative, the body diode in the transistor will conduct the voltage to ground. In reality, a diode has a voltage drop due to its nonlinear behavior. For this model, an ideal diode that conducts for all negative voltages will be assumed. The impact on the FFT will be similar, as it 'throws away' information in the negative part of the waveform.

Because of the pulse-like shape of the waveform, the body diode can have effect at 3 places in the waveform. The first possibility is that the waveform starts with a negative voltage. The diode will conduct until the waveform becomes positive. In real situations, this event will never take place, as this would assume that as soon as the switch opens, a current *from* the load charges the inductance. This means that energy is taken from the load instead of energy delivered to the load and that the impedance of the load would be negative.

The second possibility is that the waveform becomes negative in the middle of the wave. In this assignment, is it assumed that the ideal diode conducts all energy and that a negative voltage becomes zero as long as the voltage remains negative. This is illustrated by Fig. 5.2.

The third option is that the waveform becomes negative at the end of the waveform, which happens if the α-parameter is negative. This is shown in Fig. 5.3. In this event, something different occurs. Because of the negative voltage, the diode conducts, which can be seen as if the switch opens. Because the next cycle starts with the switch opened, effectively the next cycle has starter earlier and the duty cycle d of this cycle has increased. This is illustrated by Fig. 5.4. Because now the coil has more time to charge, the voltage and current behavior of the next cycle will be influenced. Therefore the *matlab* model has been modified to extend the duty cycle when this event occurs.

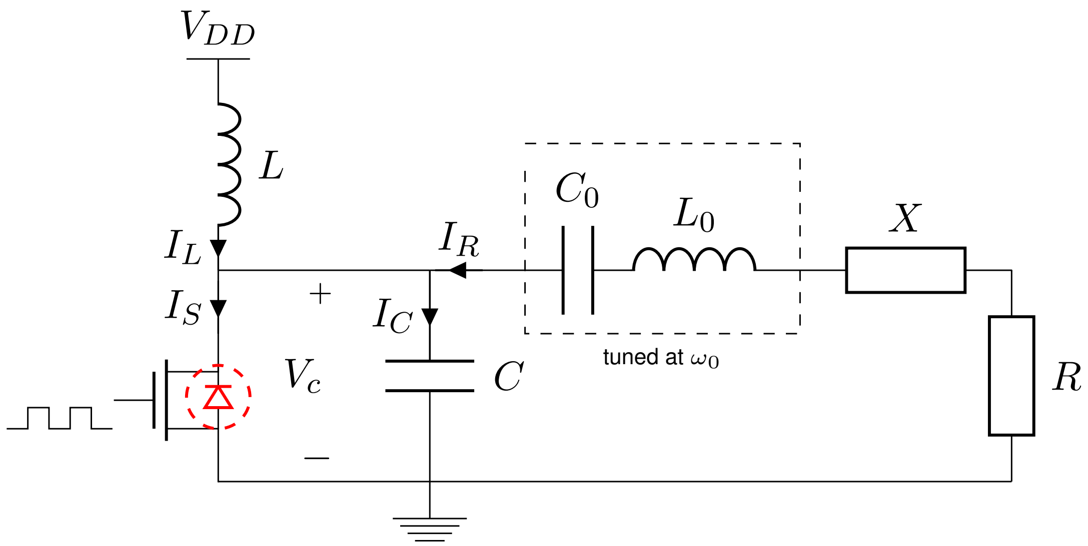

Figure 5.1: Body diode of a FET.

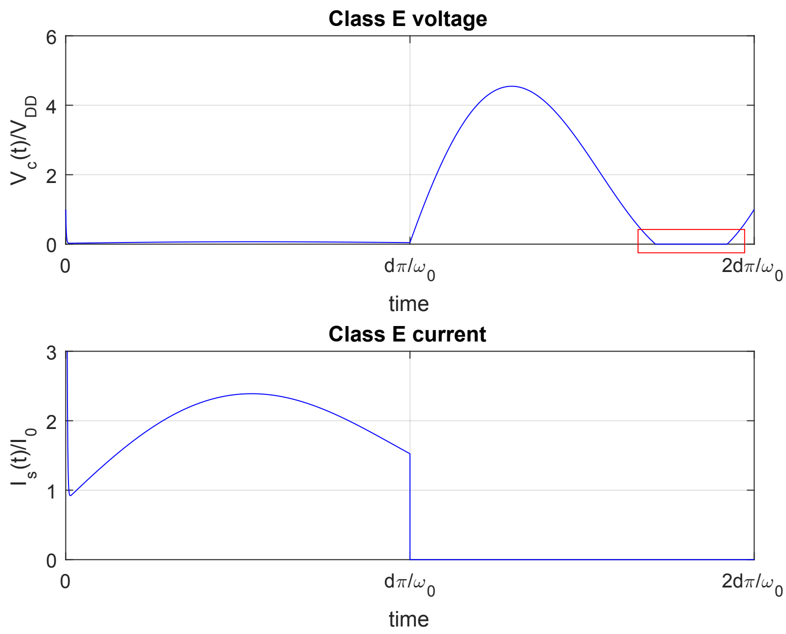

Figure 5.2: Diode effect in middle of a waveform

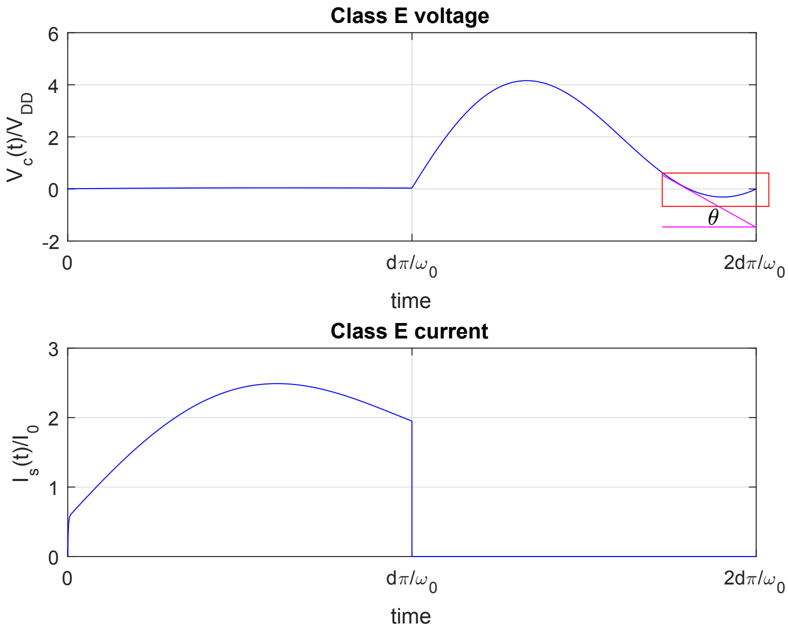

Figure 5.3: Negative V_C at the end of the cycle. For the diode simulation, the period in which V_C is negative at the end of the cycle will be added to the dutycycle. α is now 0 and β is $\tan(\theta)$.

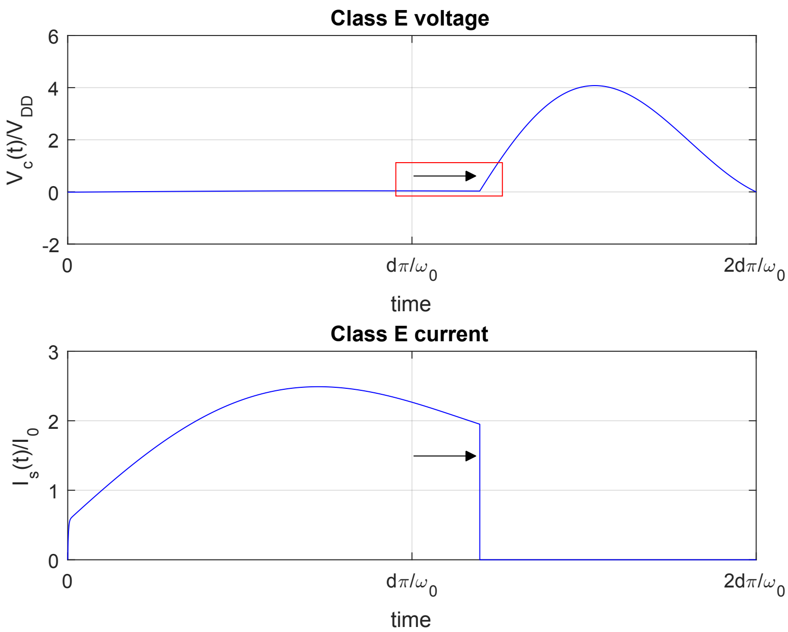

Figure 5.4: Corrected waveform: wave is moved and d has increased

5.2 Simulation model

When a negative voltage is found at the end of a cycle, the simulation is redone with a duty cycle that is extended by exactly the amount of time that the diode was conducting, and an α-parameter of 0, as the cycle now ends at the zero crossing. Also the β-parameter is modified so that it is equal to $\frac{dV(t)}{dt}$ with t the time the diode start conducting as shown in Fig. 5.3.

As the situation in which the duty cycle is increased as the result of the diode conducting at the end of a duty cycle occurs whenever α is zero, meaning that this occurs at approximately half of the Γ_Z-plane. Moreover, because this behavior removes a lot of information of the waveform and therefore also information for the harmonics it is important to examine the effects on the accuracy. Fig. 5.5 shows at which loads the diode conducts on a Smith Chart.

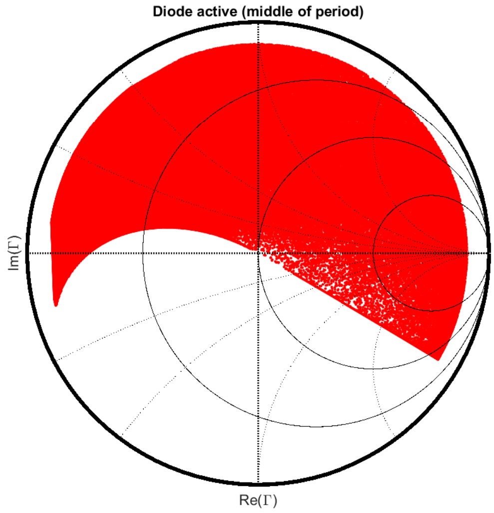

Diode effect in middle of a waveform.

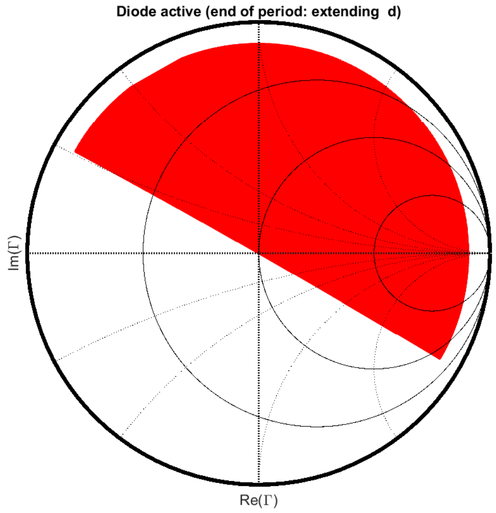

Diode effect in the end of waveform.

Figure 5.5: Smith Chart showing values of Γ_Z for which the body diode of the switch conducts, changing the waveform of V_C.

6. Performance with diode

6.1 Simulations, gradient and combinations

The simulations for the set of α and β values is now repeated with these diode effect as described in the previous section. The resulting contour plots and gradients are shown in Figs. D.1 to D.5 in Appendix D and in Figs. E.1 to E.9 in Appendix E. It can be seen that is is much harder now to perform an estimation in the $\alpha < 0$ area. Numerical values of the mean gradient and mean error sensitivity are shown in Tables 6.1 and 6.2.

Table 6.1: Mean gradient amplitude for different complex harmonic content variables in $\frac{1}{1 \times 10^3}$ $(\frac{1}{\Gamma_Z})$

	Amplitude	Phase	Re	Im
0th	-	-	135.3470	-
1st	123.3953	0.1855	283.5382	93.3211
2nd	176.2898	1.3758	109.1925	320.6371
3rd	154.9755	0.7446	146.5969	112.7021
4th	70.1014	1.6628	65.4913	23.8266
5th	34.3643	0.8134	37.8172	26.0273
6th	18.6803	1.4381	8.1017	23.4768

Table 6.2: Mean noise error in in 1×10^{-3} (Γ_Z), optimal direction for 1 $\frac{V}{V_{dd}}_{pp}$ Additive White Gaussian Noise. The numbers represent the mean deviation in reflection factor for AWGN: a lower number means that the parameter is less sensitive for noise on V_C.

	Amplitude	Phase	Re	Im
0th	-	-	0.0760	-
1st	0.0590	0.0300	0.0257	0.0779
2nd	0.0413	0.0108	0.0666	0.0227
3rd	0.0470	0.0202	0.0496	0.0646
4th	0.1038	0.0478	0.1111	0.3054
5th	0.2117	0.0470	0.1924	0.2797
6th	0.3887	0.0930	0.8983	0.3100

6.2 Combinations

With the gradients, again the combinations can be calculation. The graphical results is shown in Fig. 6.1, the full table with numerical results is shown in Table F.1 in Appendix F. A subset of this table containing the 6 largest combined sensitivity values is shown in Table 6.3.

Table 6.3: Mean combined sensitivity value $C_{nm} \times 10^7$ for different combinations of harmonics. Subset of the complete Table F.1 in Appendix F. The combination with the six largest values are shown in gray. Note that these results differ from the results without diode in Table 6.3.

	h_{2p}	h_{2i}	h_{3p}
h_{1a}	0.94	0.64	0.78
h_{1p}	0.69	0.34	0.82
h_{1i}	0.81	0.71	0.82
h_{2a}	1.07	0.49	0.74
h_{2p}	-	0.65	1.10
h_{2r}	0.74	0.87	1.69

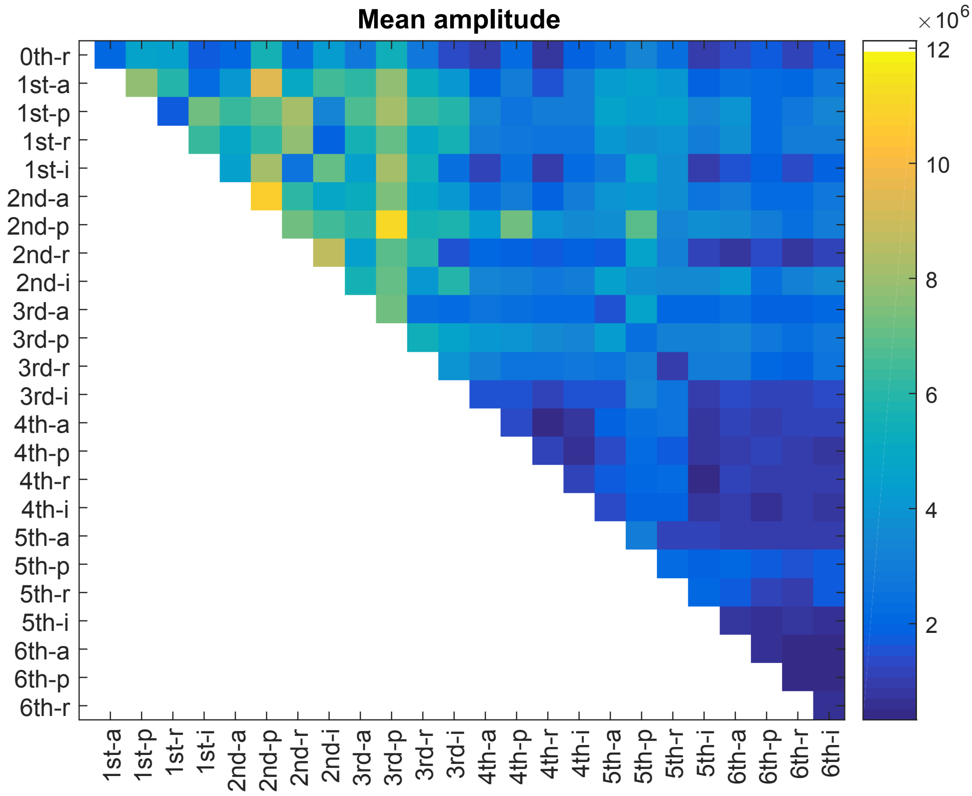

Figure 6.1: Color plot with the sensitivity values of all combinations. A higher value means less error sensitivity. A table with all numerical values can be found in Table C.1 in Appendix C.

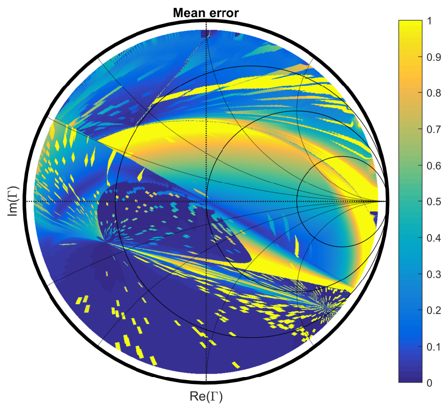

h_{2p} and h_{3p}

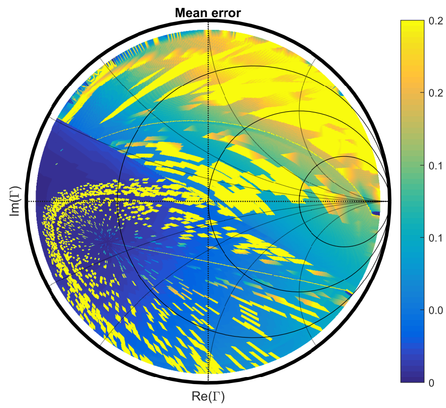

h_{2a} and h_{2p}

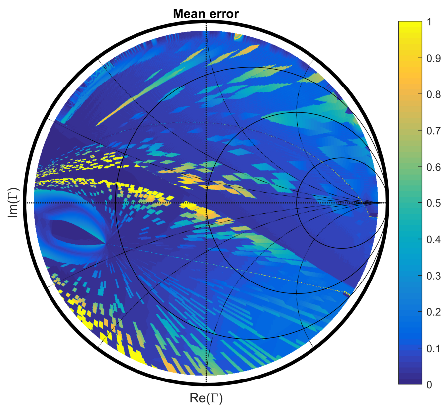

h_{1a} and h_{2p}

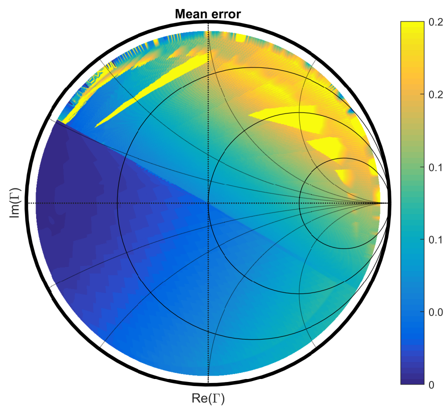

h_{2r} and h_{2i}

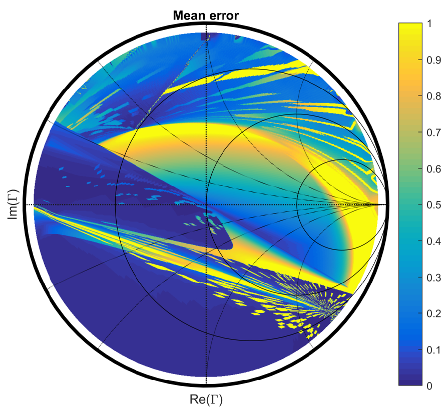

h_{1p} and h_{3p}

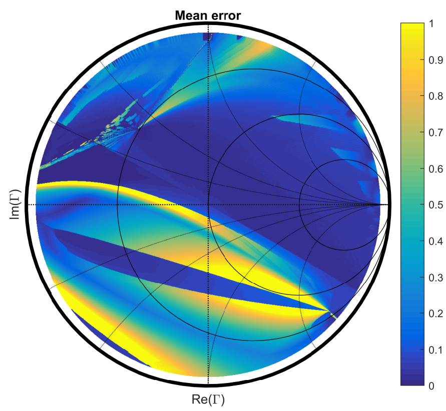

h_{1i} and h_{3p}

Figure 6.2: Maximum Γ_Z error for an offset in harmonic parameters caused by AWGN 1 $\frac{V}{V_{dd\ pp}}$ distortion, when estimation Γ_Z by use of different combinations of harmonic parameters.

6.3 Testbench

To test the performance of the estimation technique with an amplifier model with body diode the testbench is used again with lookup tables built with a model that includes a body diode. In Fig. 6.3 the testbench results of the six best performing combinations are shown, for $\alpha = 0$ and $\beta = 0$. As predicted by the estimated error calculation, results are generally worse than the model without the diode. Especially the combinations h_{2r}-h_{2i} and h_{1i}-h_{3p}, which show load estimations far away from the actual used load.

Finally, a testbench simulation for multiple values of α and β is done for the h_{2p} and h_{3p} combination, as this combination gives the highest combined sensitivity value of all compared combinations. The Smith chart showing the results is shown in Fig. 6.4. To increase the change of finding an estimated load impedance, the noise level is lowered to $0.1\frac{V}{V_{DD\,pp}}$. fluctuations of the values in the lookup tables are that high, that no estimated load impedances can be found for values of Γ_Z where $\alpha < 0$. The testbench is repeated for h_{2a} + h_{2p} and h_{1a} + h_{2p}, but these combinations give similar results. Unfortunately load impedance estimation using this diode extension technique and these lookup tables did not succeed for $\alpha < 0$.

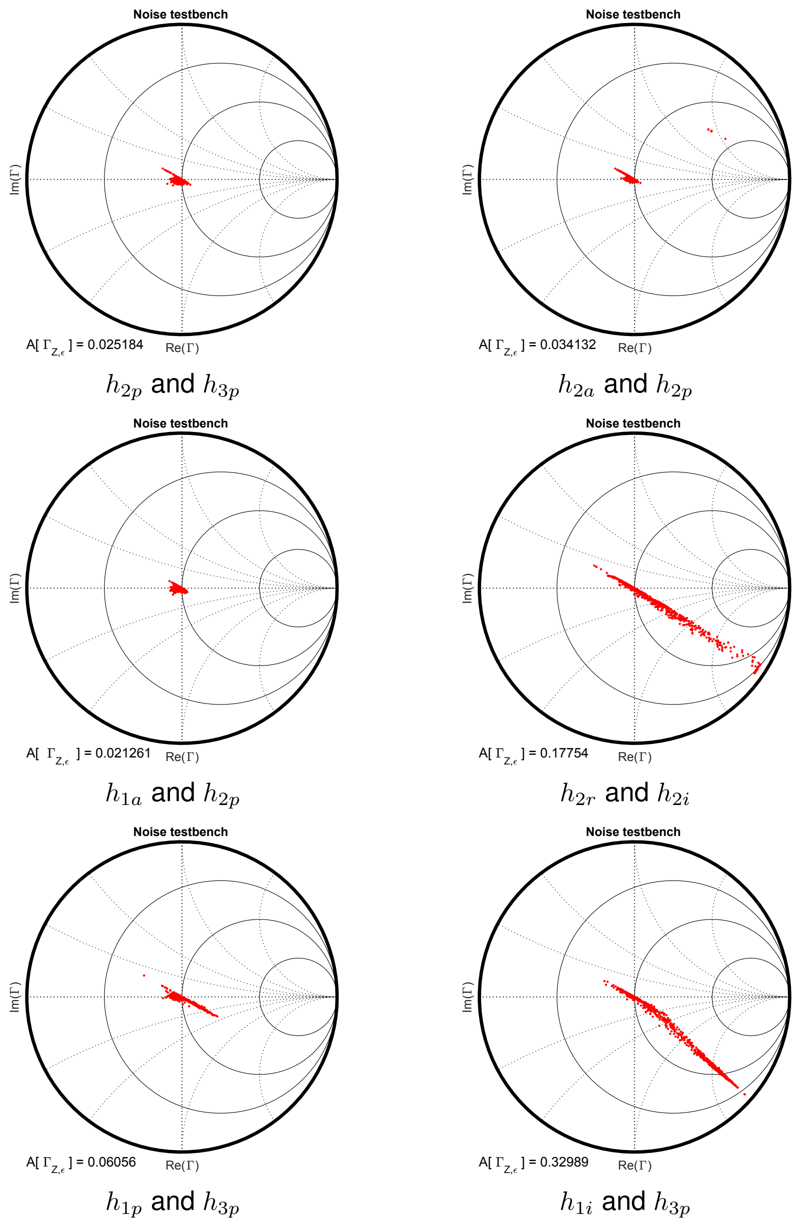

Figure 6.3: Performance of the load estimation by AWGN 1 $\frac{V}{V_{dd\,pp}}$ distortion for $\alpha = 0$ and $\beta = 0$ and a combination of two harmonic parameters. Different combinations of harmonic parameters for load estimation are shown. For each combination the mean error A $[\Gamma_{Z,\epsilon}]$ is specified.

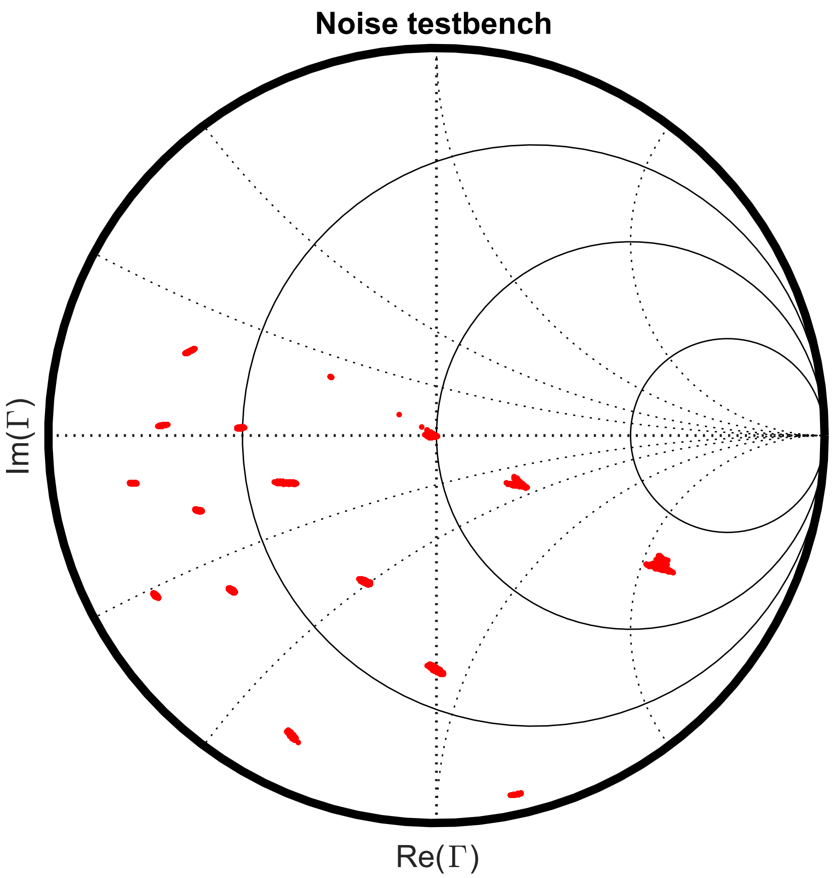

Figure 6.4: Noise testbench results for multiple values of α and β ($\alpha = \{-6, -4, -2, 0, 2, 4, 6\}$, $\beta = \{-2, -1, 0, 2, 4, 8\}$), using a combination of h_{2p} and h_{3p}, that gave the highest combined sensitivity value. The blue dots represent the actual impedance, the red dots the estimated instances with $0.1\frac{V}{V_{DD}}_{pp}$ AWGN.

7. Conclusion

To perform a load estimation for Class E RF power amplifiers using the harmonic content of the voltage waveform of the switch node, lookup tables for the first six harmonics and DC are build. As harmonics are complex valued, every harmonic gives two parameters. When these complex parameters are described as amplitude and angle, two more parameters can be distinguished resulting in a total of four parameters per harmonic.

The lookup tables are investigated for accuracy and the amount of information a table gives about the load, given a certain measurement accuracy and noise. For each harmonic parameter, the gradient, as measure of sensitivity, noise sensitivity and mean noise error are calculated. These values can tell that the DC component of the signal does not provide much information, and results in large estimation errors. Furthermore, the lower harmonic provide more information than higher harmonics.

As one parameter does not give enough information to estimate a complex valued load impedance, simulations are done to calculate the performance of the use of combinations of two lookup tables. These calculations conclude that not only the sensitivity and error of a harmonic parameter is important, but also the direction in which these properties are of great importance. The results show that combinations of harmonics that individually seems to deliver most information, do not give as much information as parameters that have a sensitivity that is more orthogonal.

The performance of an estimation testbench, using the calculated lookup tables, is tested, by adding different instances of noise to a simulated voltage waveform. The testbench shows that it is possible to estimate a load impedance with great accuracy, even if a lot of noise it added to the measured signal.

The body diode in the switching element distorts the voltage waveform heavily, resulting in larger errors in the estimation process, especially when $\alpha < 0$, but also for all other load impedances. The results show that there are a lot of spots on the Γ_Z-plane where the estimation error is very high, even when multiple harmonic parameters are combined to find the best estimated load impedance.

When the testbench was used to test the performance of the load impedance estimation with this diode effect included in the simulation, the testbench could not estimate impedances for which $\alpha < 0$, because the lookup tables show lots of irregularities due to the diode.

Because the model uses a very basic model of a diode, namely that it prevents all negative voltages over the capacitor, the performance is possibly worse than when a real body diode is used, as the reverse voltage has a certain threshold, allowing a small negative voltage dependent on the used technology.

The results thus show that estimating the load impedance, based on the harmonic content of the voltage at the switching element in a Class-E RF amplifier is possible, and has an acceptable accuracy, as long as the effect of the body diode can be neglected. This is of course not the case. When this is not neglected, estimations for load impedances where $\alpha < 0$ need very accurate measurements and lookup tables. Because a very simplistic model of this diode is used, the simulated performance is possibly worse than the performance with a more accurate model.

Bibliography

[1] Mustafa Acar. *Power Amplifiers in CMOS technology*. 2011.

[2] Mustafa Acar, Anne Johan Annema, and Bram Nauta. Generalized analytical design equations for variable slope class-e power amplifiers. In *2006 13th IEEE International Conference on Electronics, Circuits and Systems*, pages 431–434. IEEE, 2006.

[3] Mustafa Acar, Anne Johan Annema, and Bram Nauta. Analytical design equations for class-e power amplifiers. *IEEE transactions on circuits and systems I: regular papers*, 54(12):2706–2717, 2007.

[4] Bram Nauta Ali Ghahremani, Anne-Johan Annema. Load-mismatch sensitivity of class-e power amplifiers. -, March 2016.

[5] Steve C. Cripps. *RF Power Amplifiers for Wireless Communications*. 1999.

[6] Maikel Huiskamp. Rf-waveform characterization for self-healing rf power amplifiers. -, December 2015.

[7] Thomas H. Lee. *The Design of CMOS Radiofrequency Integrated Circuits*. 1998.

[8] Berjan Westerdijk. Design of a self-healing class-e amplifier testbed, 2016.

A. Harmonic parameter plots

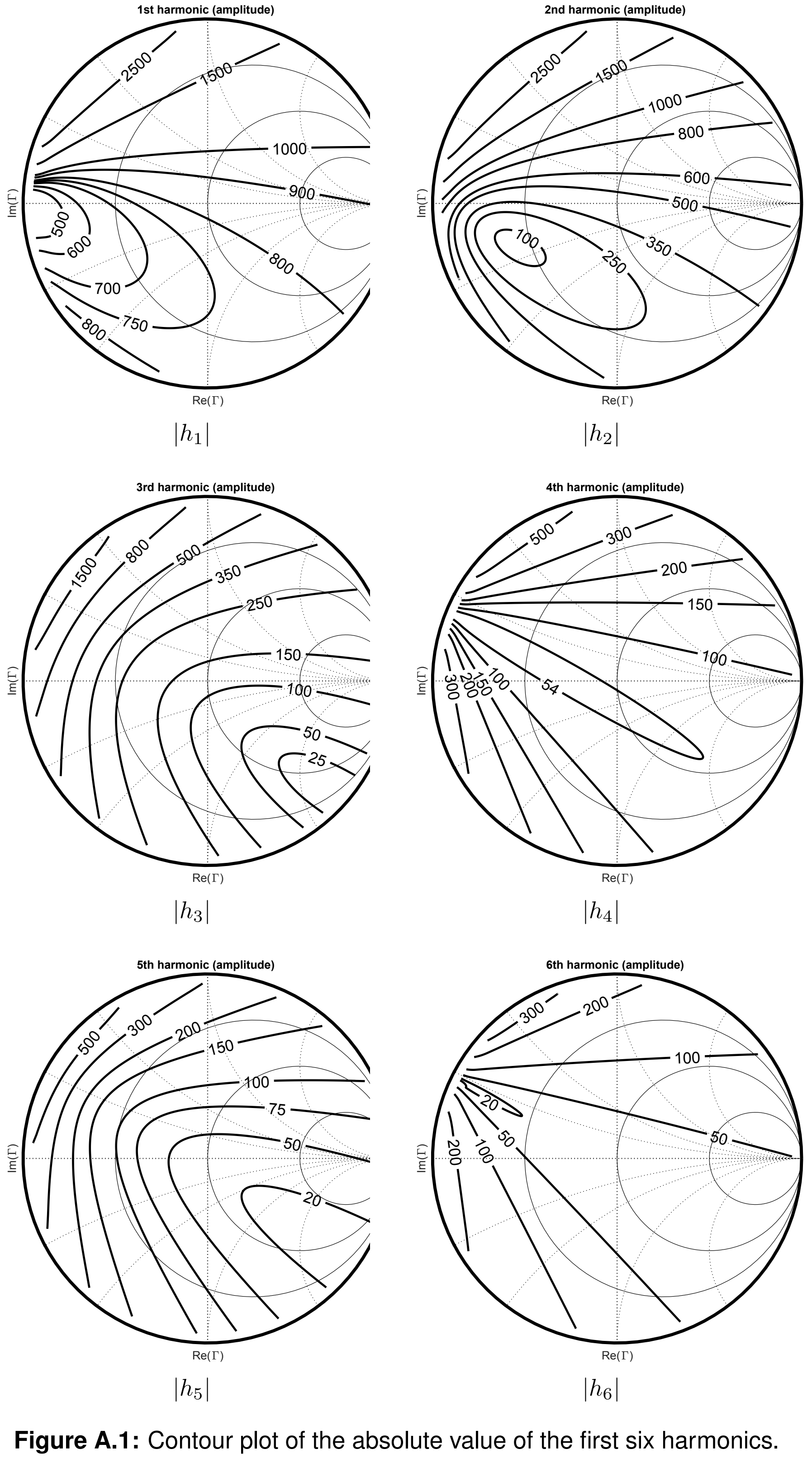

Figure A.1: Contour plot of the absolute value of the first six harmonics.

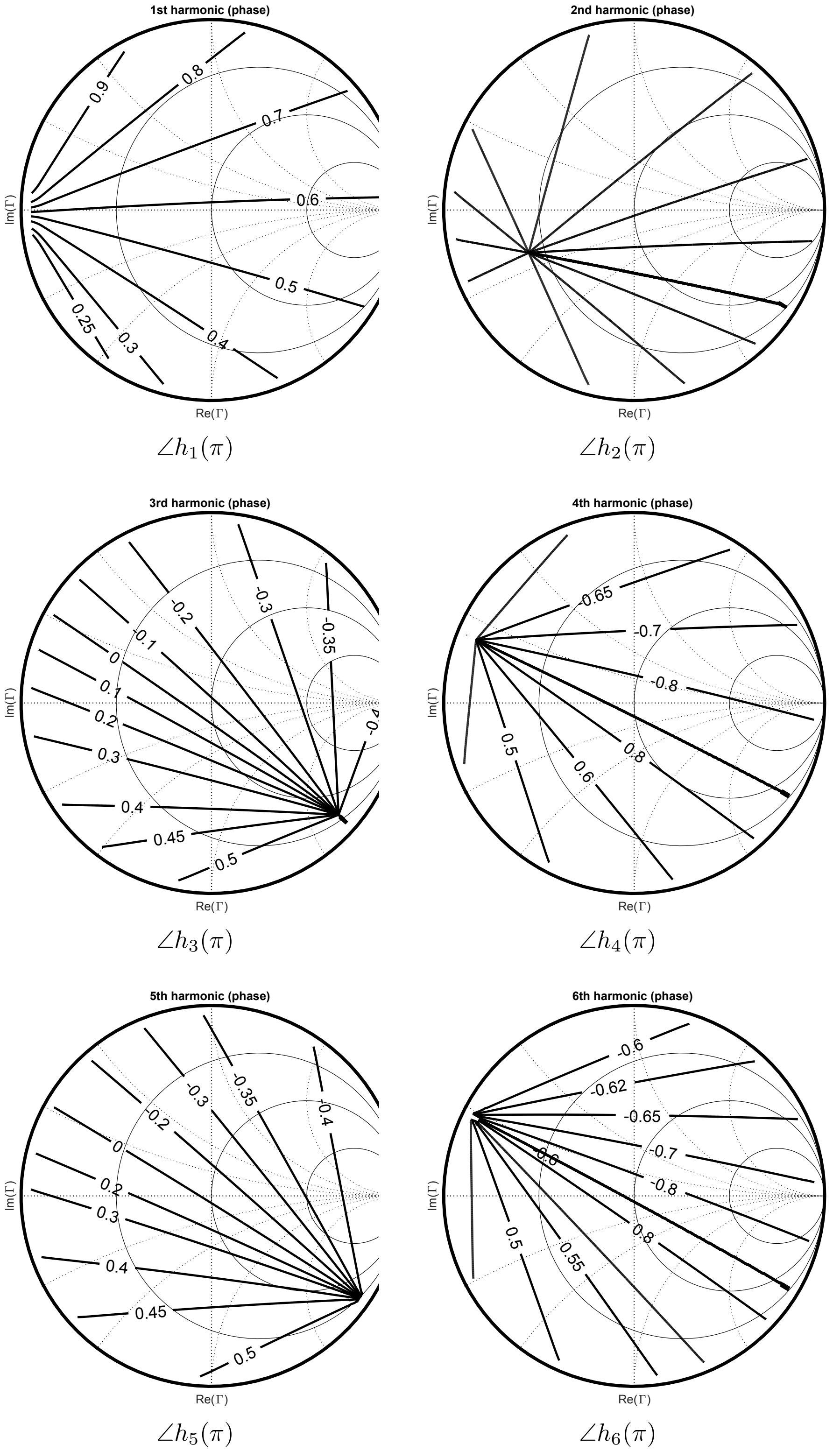

Figure A.2: Contour plot of the complex angle of the first six harmonics.

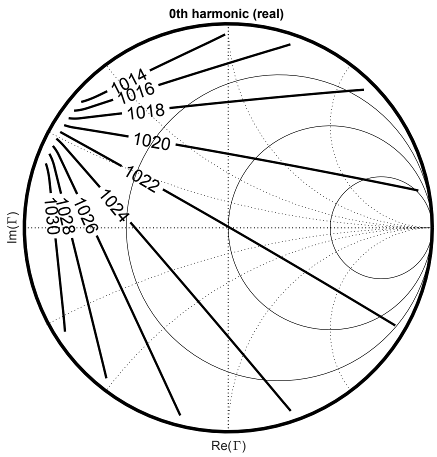

Figure A.3: Contour plot of the real part of the 0th harmonic (DC), $\mathrm{Re}\, h_0$.

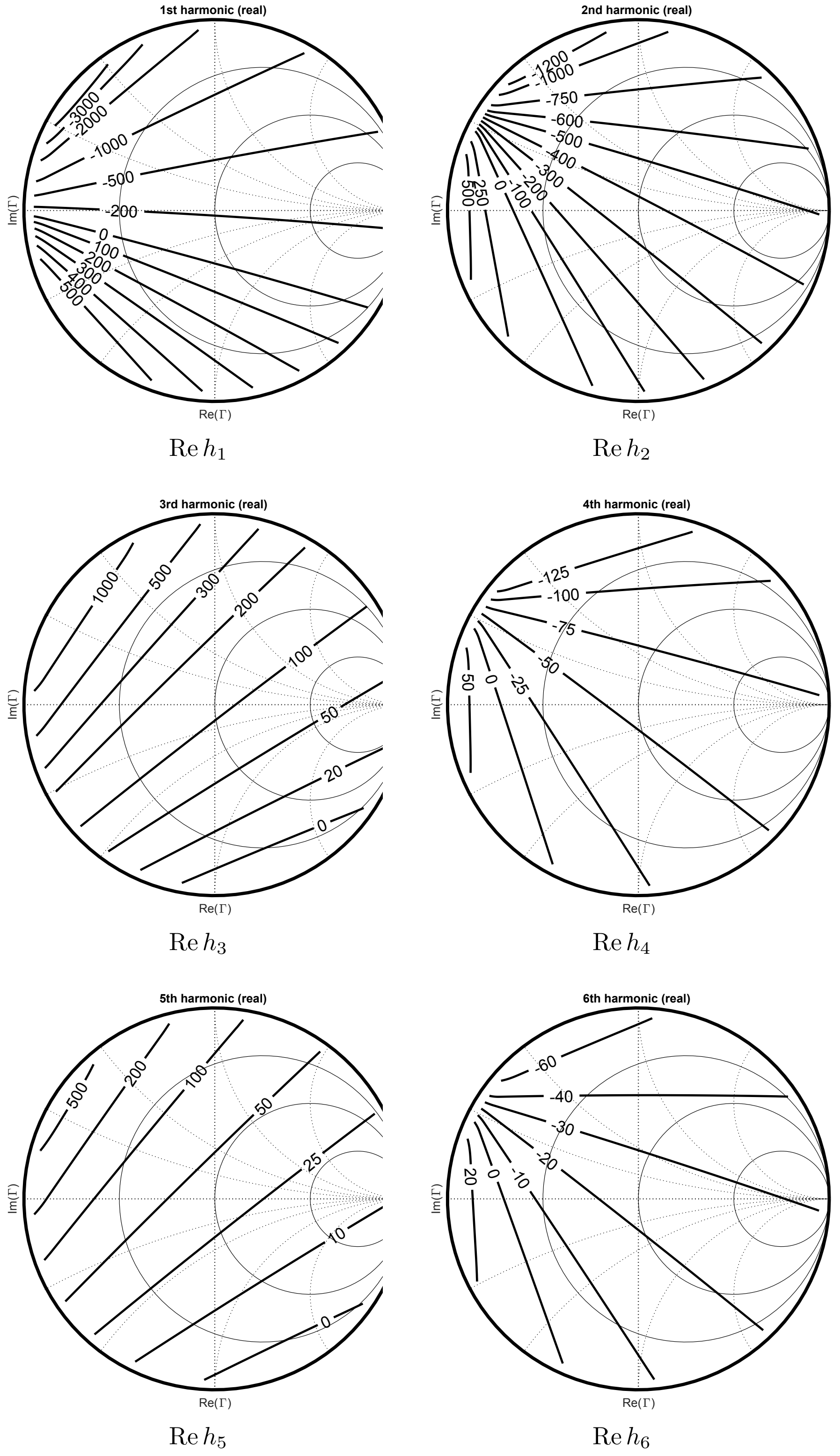

Figure A.4: Contour plot of the real part of the first six harmonics.

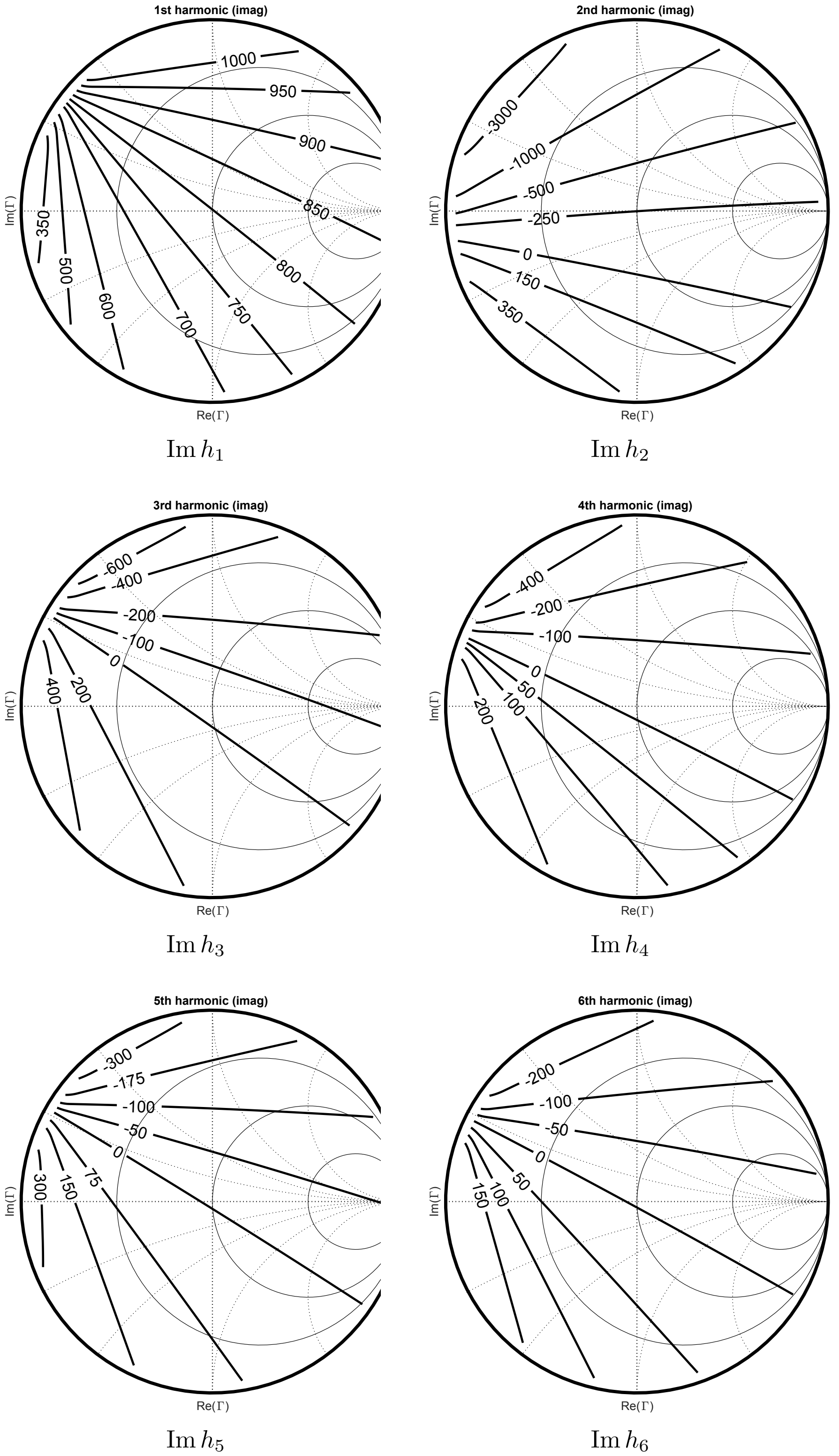

Figure A.5: Contour plot of the imaginary part of the first six harmonics.

B. Harmonic parameter gradient plots

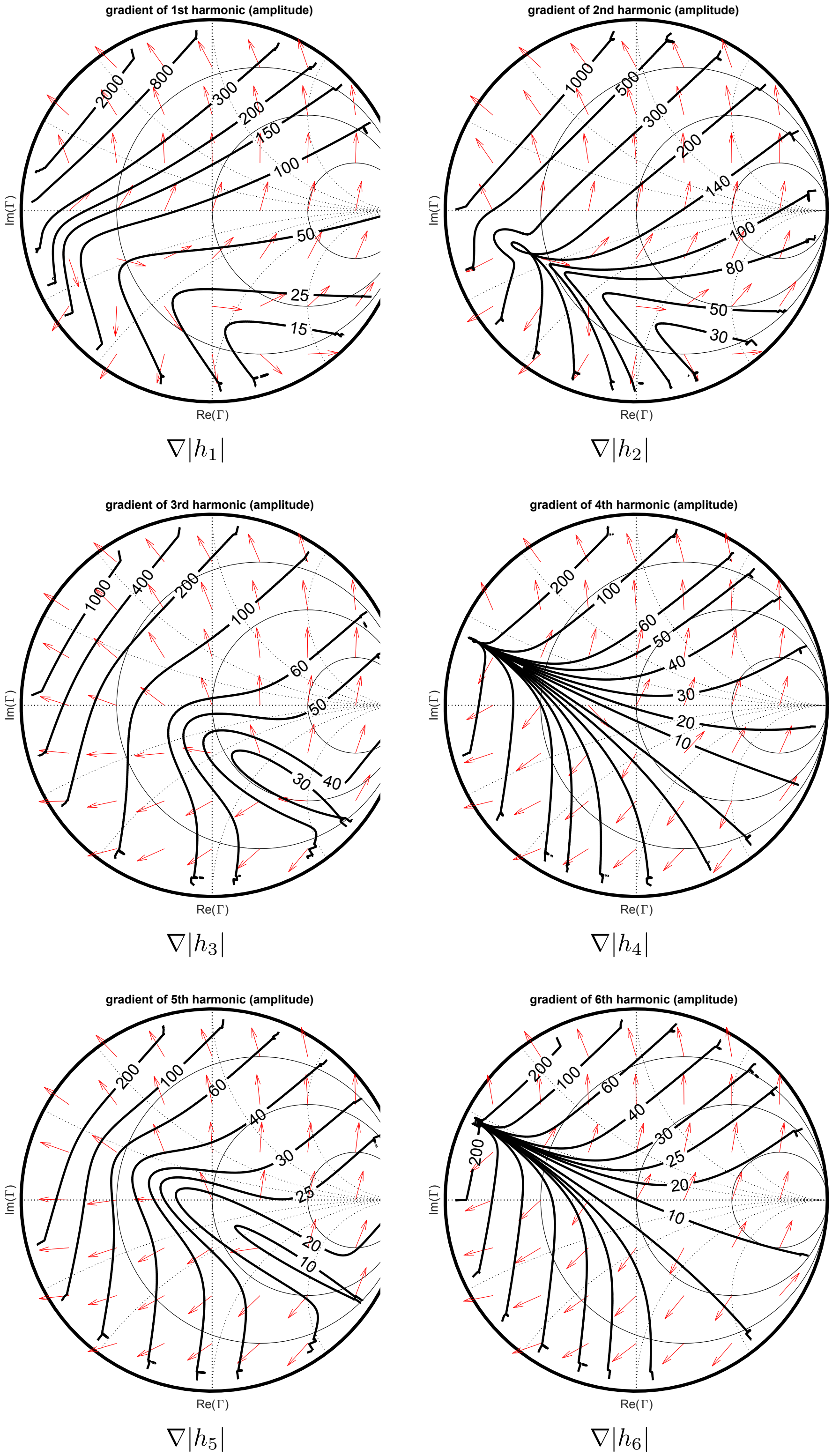

Figure B.1: Gradients of the absolute value of the first six harmonics.

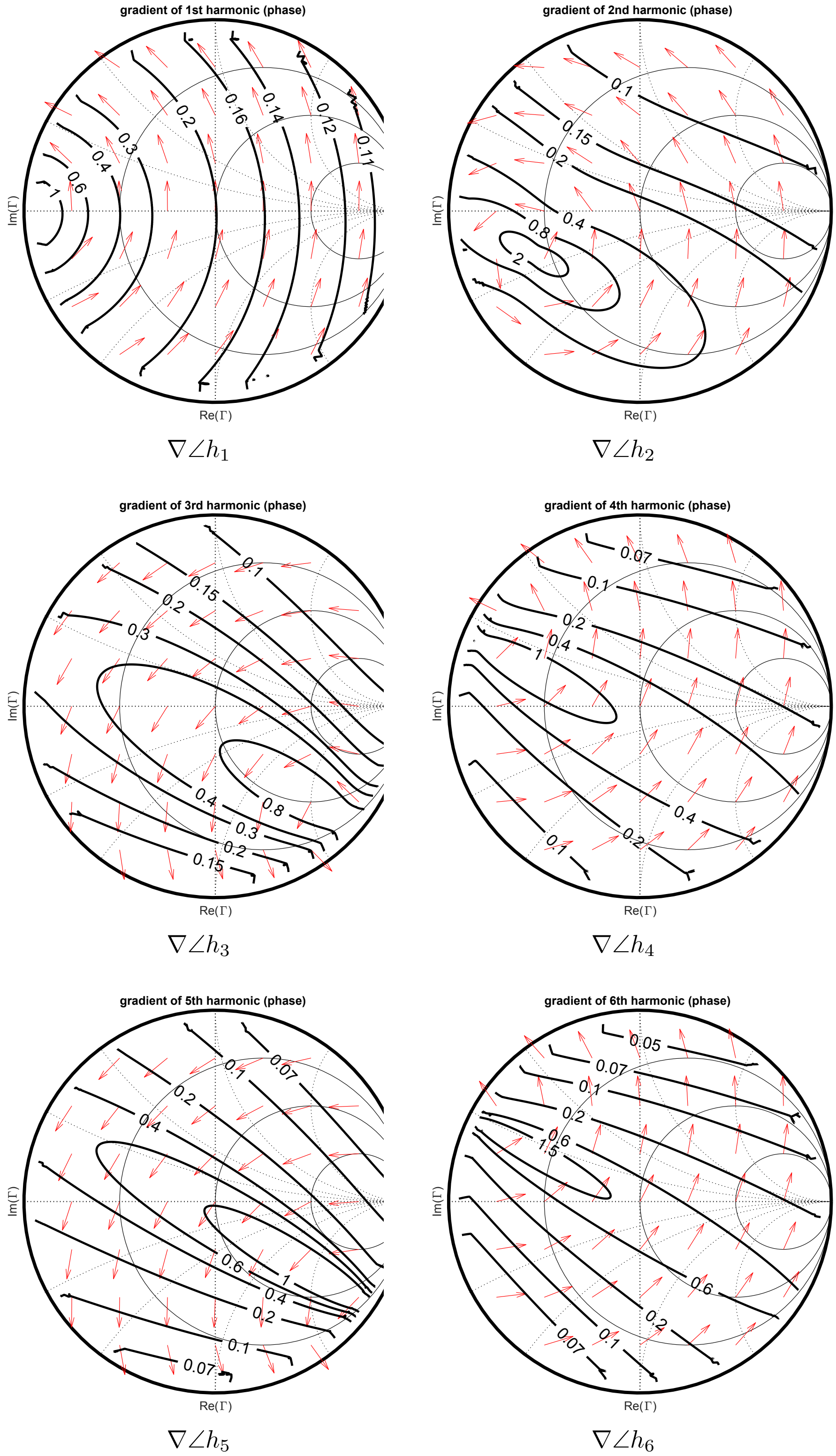

Figure B.2: Gradients of the complex phase of the first six harmonics.

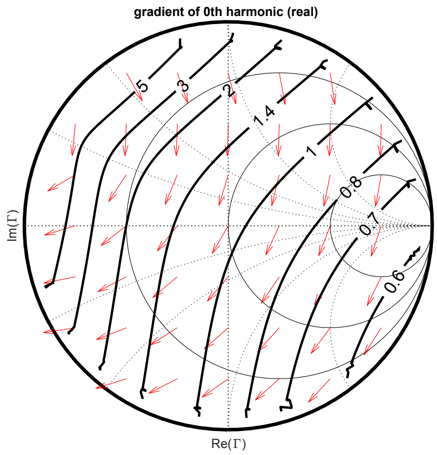

Figure B.3: Gradient of the real part of the 0th harmonic (DC), $\nabla \operatorname{Re} h_0$.

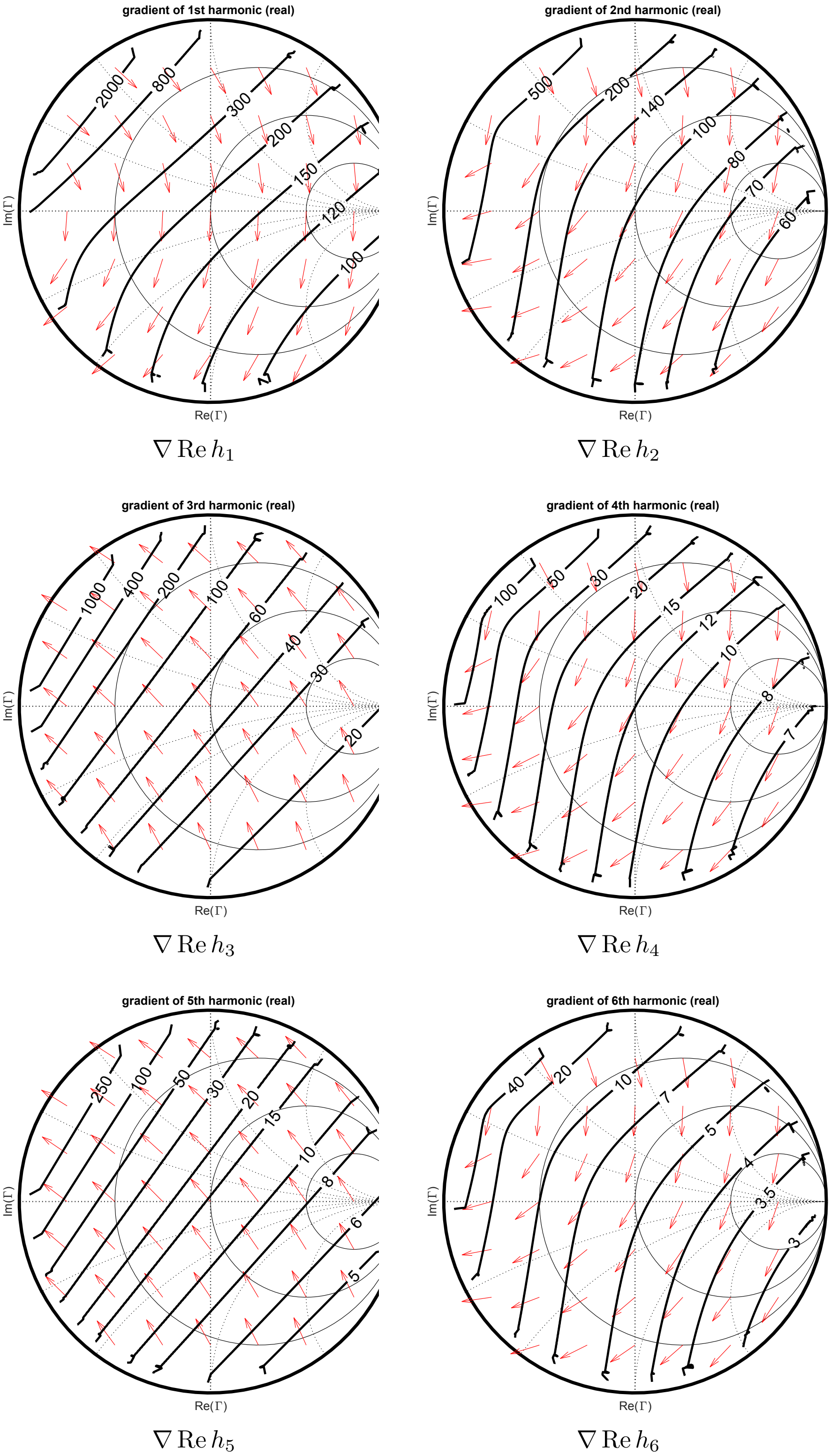

Figure B.4: Gradients of the real part of the first six harmonics.

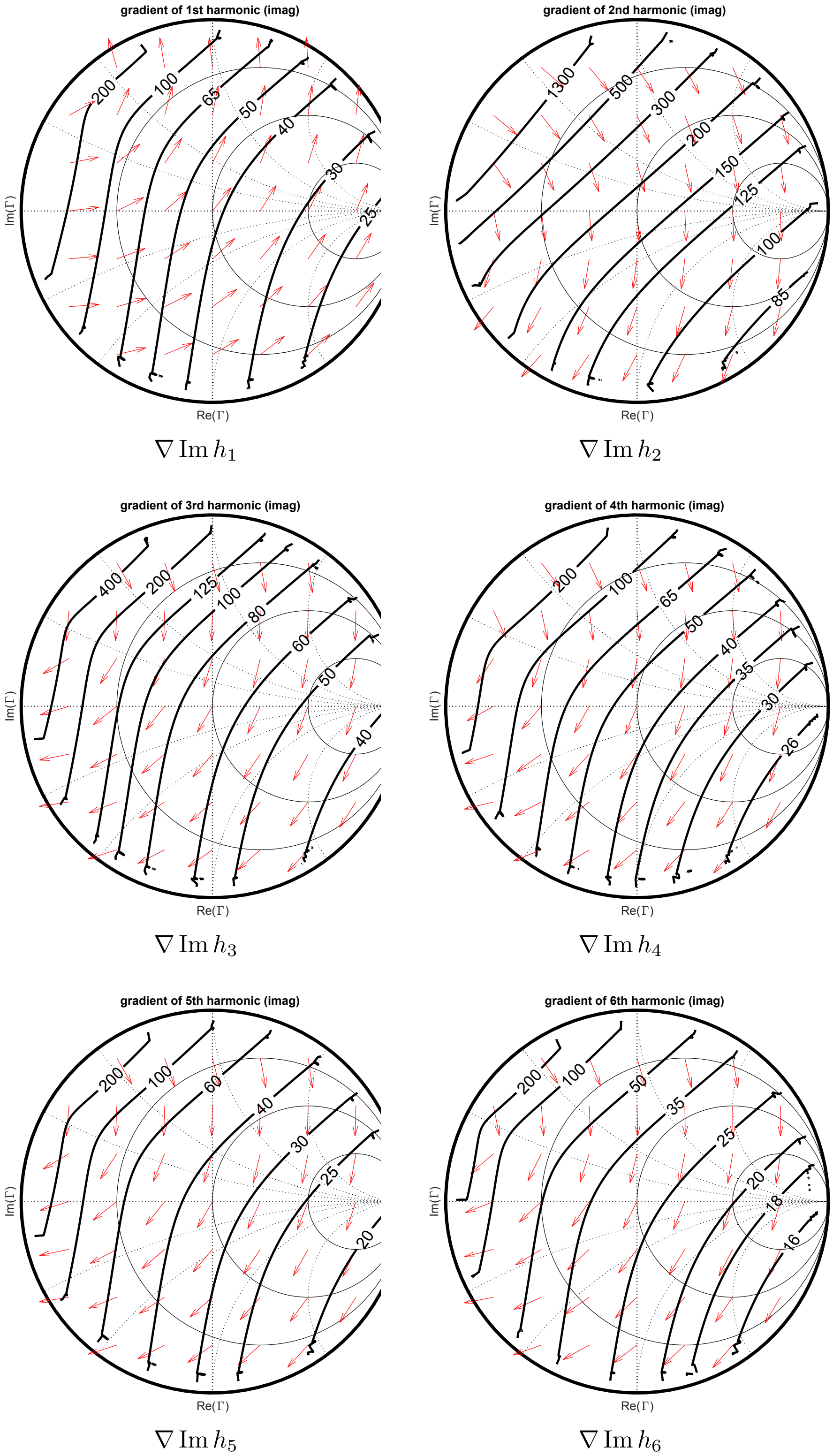

$\nabla\, \mathrm{Im}\, h_1$ $\nabla\, \mathrm{Im}\, h_2$

$\nabla\, \mathrm{Im}\, h_3$ $\nabla\, \mathrm{Im}\, h_4$

$\nabla\, \mathrm{Im}\, h_5$ $\nabla\, \mathrm{Im}\, h_6$

Figure B.5: Gradients of the imaginary part of the first six harmonics.

C. Harmonic parameter combinations

Table C.1: Combined sensitivity value $C_{nm} \times 10^7$ for all combinations between harmonic parameters as defined in Section 4.3. The top 6 combinations that are further discussed in this section are marked in gray. A: Amplitude, P: Phase, R: Real part, I: Imaginary part.

1A	1P	1R	1I	2A	2P	2R	2I	3A	3P	3R	3I	4A	4P	4R	4I	5A	5P	5R	5I	6A	6P	6R	6I	
0.09	0.11	0.12	0.02	0.11	0.08	0.00	0.13	0.07	0.08	0.10	0.00	0.02	0.01	0.00	0.02	0.03	0.05	0.06	0.00	0.01	0.00	0.00	0.01	**0R**
-	0.92	0.48	0.84	0.45	1.01	1.05	0.67	0.70	1.05	0.87	0.85	0.52	0.24	0.37	0.51	0.41	0.67	0.49	0.60	0.47	0.22	0.24	0.48	**1A**
-	-	0.42	0.93	0.73	0.98	1.25	0.45	0.76	1.31	0.84	1.02	0.65	0.43	0.44	0.69	0.55	0.80	0.48	0.72	0.57	0.36	0.29	0.61	**1P**
-	-	-	1.09	0.46	1.01	1.39	0.36	0.83	1.36	1.02	1.12	0.67	0.39	0.49	0.69	0.55	0.85	0.58	0.80	0.61	0.35	0.32	0.65	**1R**
-	-	-	-	0.98	0.63	0.20	1.17	0.56	0.59	0.77	0.19	0.26	0.15	0.07	0.28	0.26	0.35	0.42	0.13	0.15	0.09	0.05	0.16	**1I**
-	-	-	-	-	1.37	1.27	0.54	0.68	1.38	0.90	1.03	0.65	0.33	0.45	0.65	0.44	0.87	0.51	0.73	0.57	0.31	0.30	0.60	**2A**
-	-	-	-	-	-	0.90	1.01	0.80	1.04	0.72	0.75	0.51	0.39	0.32	0.57	0.53	0.62	0.40	0.53	0.43	0.30	0.21	0.46	**2P**
-	-	-	-	-	-	-	1.55	0.83	0.89	1.15	0.03	0.21	0.15	0.00	0.23	0.37	0.52	0.64	0.02	0.08	0.06	0.00	0.09	**2R**
-	-	-	-	-	-	-	-	0.78	1.40	0.85	1.26	0.80	0.45	0.54	0.83	0.58	0.89	0.49	0.90	0.71	0.40	0.36	0.74	**2I**
-	-	-	-	-	-	-	-	-	1.19	0.43	0.69	0.50	0.28	0.29	0.53	0.16	0.74	0.24	0.49	0.40	0.25	0.19	0.43	**3A**
-	-	-	-	-	-	-	-	-	-	0.95	0.74	0.55	0.41	0.31	0.60	0.71	0.19	0.53	0.53	0.44	0.29	0.21	0.47	**3P**
-	-	-	-	-	-	-	-	-	-	-	0.95	0.69	0.40	0.40	0.73	0.40	0.64	0.01	0.68	0.56	0.33	0.27	0.60	**3R**
-	-	-	-	-	-	-	-	-	-	-	-	0.15	0.12	0.01	0.17	0.31	0.43	0.53	0.00	0.05	0.05	0.01	0.06	**3I**
-	-	-	-	-	-	-	-	-	-	-	-	-	0.08	0.07	0.02	0.23	0.32	0.38	0.11	0.05	0.04	0.05	0.05	**4A**
-	-	-	-	-	-	-	-	-	-	-	-	-	-	0.05	0.07	0.14	0.24	0.22	0.08	0.05	0.05	0.04	0.06	**4P**
-	-	-	-	-	-	-	-	-	-	-	-	-	-	-	0.08	0.13	0.18	0.22	0.01	0.03	0.02	0.00	0.03	**4R**
-	-	-	-	-	-	-	-	-	-	-	-	-	-	-	-	0.24	0.35	0.40	0.12	0.06	0.04	0.05	0.06	**4I**
-	-	-	-	-	-	-	-	-	-	-	-	-	-	-	-	-	0.45	0.22	0.22	0.18	0.12	0.09	0.19	**5A**
-	-	-	-	-	-	-	-	-	-	-	-	-	-	-	-	-	-	0.35	0.30	0.26	0.17	0.12	0.27	**5P**
-	-	-	-	-	-	-	-	-	-	-	-	-	-	-	-	-	-	-	0.37	0.31	0.19	0.15	0.33	**5R**
-	-	-	-	-	-	-	-	-	-	-	-	-	-	-	-	-	-	-	-	0.04	0.03	0.01	0.04	**5A**
-	-	-	-	-	-	-	-	-	-	-	-	-	-	-	-	-	-	-	-	-	0.02	0.02	0.00	**6A**
-	-	-	-	-	-	-	-	-	-	-	-	-	-	-	-	-	-	-	-	-	-	0.02	0.02	**6P**
-	-	-	-	-	-	-	-	-	-	-	-	-	-	-	-	-	-	-	-	-	-	-	0.02	**6R**

D. Harmonic parameter plots with diode

In this section the harmonic parameters (amplitude, phase, real, imaginary) of the first six harmonics and DC are plotted. As the distribution over the Γ_Z-plane is not as 'neat' as the simulations without the body diode effect, color plots are used instead of contour plots.

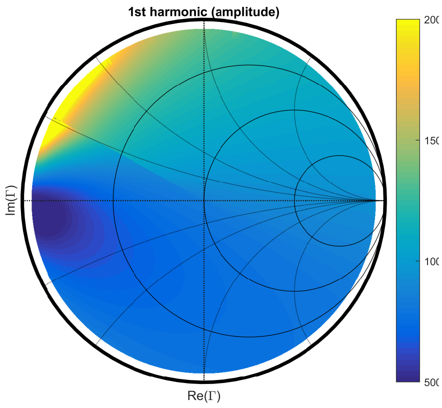

$|h_1|$

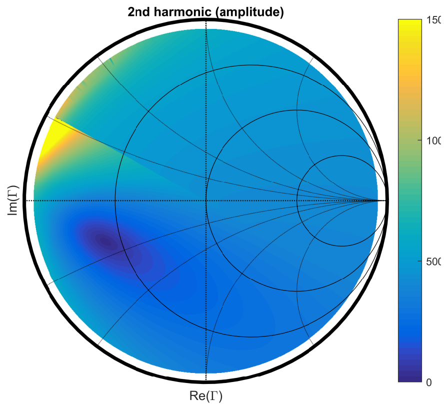

$|h_2|$

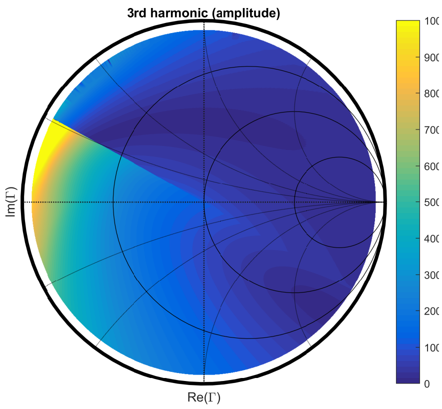

$|h_3|$

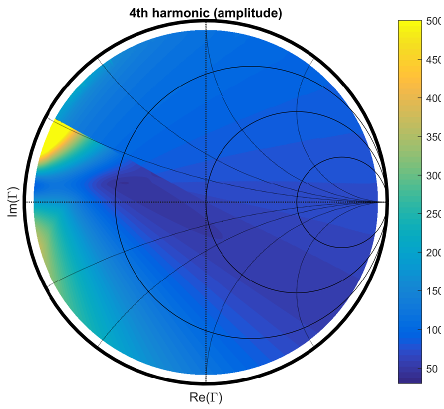

$|h_4|$

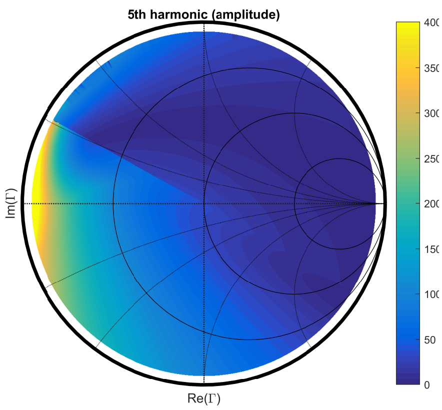

$|h_5|$

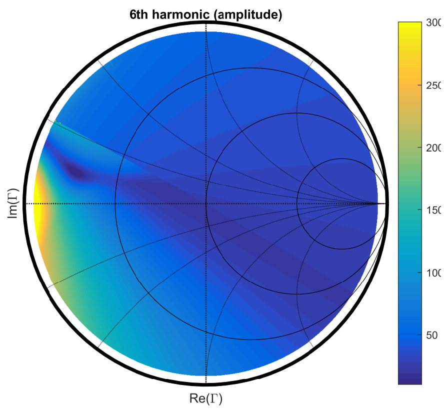

$|h_6|$

Figure D.1: Contour plot of the absolute value of the first six harmonics.

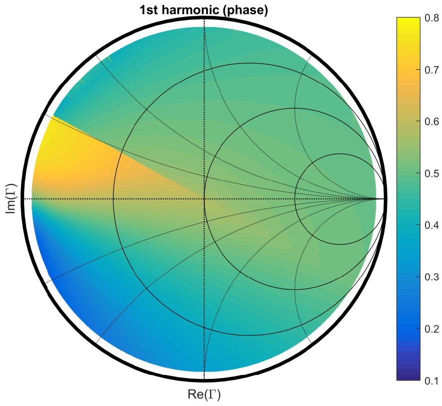

$\angle h_1(\pi)$

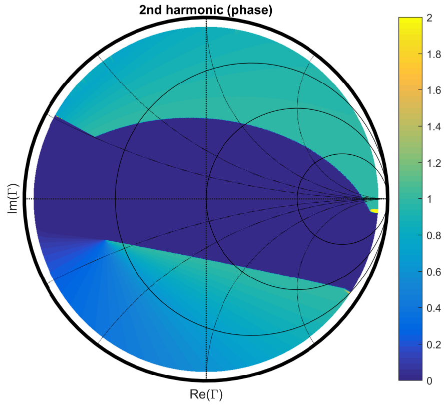

$\angle h_2(\pi)$

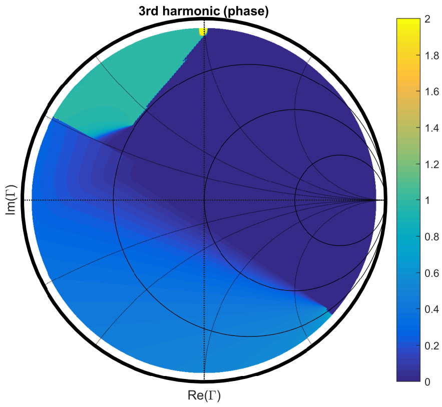

$\angle h_3(\pi)$

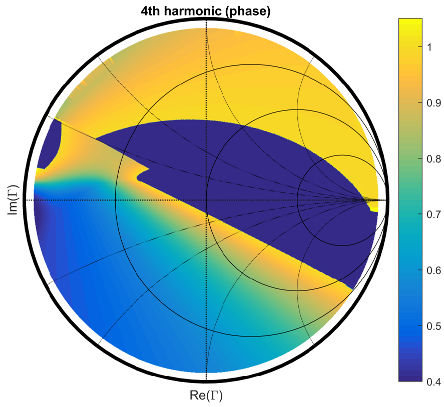

$\angle h_4(\pi)$

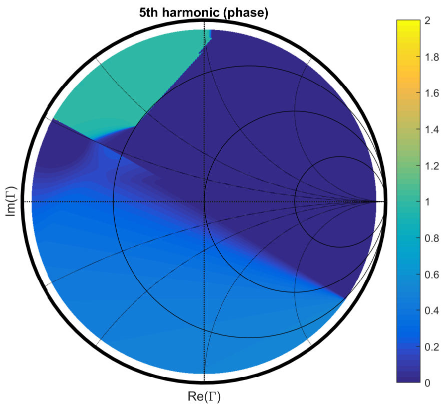

$\angle h_5(\pi)$

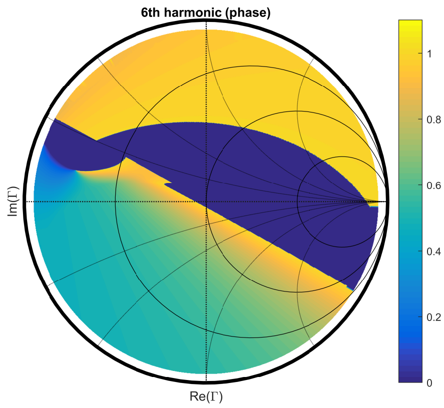

$\angle h_6(\pi)$

Figure D.2: Contour plot of the complex angle of the first six harmonics.

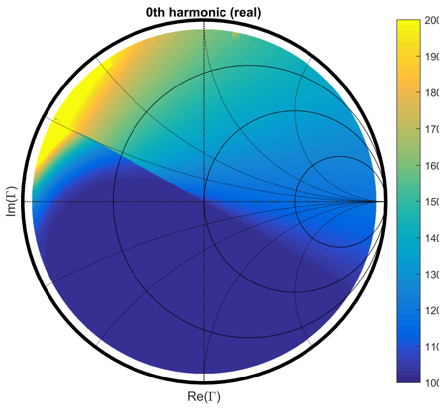

Figure D.3: Contour plot of the real part of the 0th harmonic (DC), $\mathrm{Re}\, h_0$.

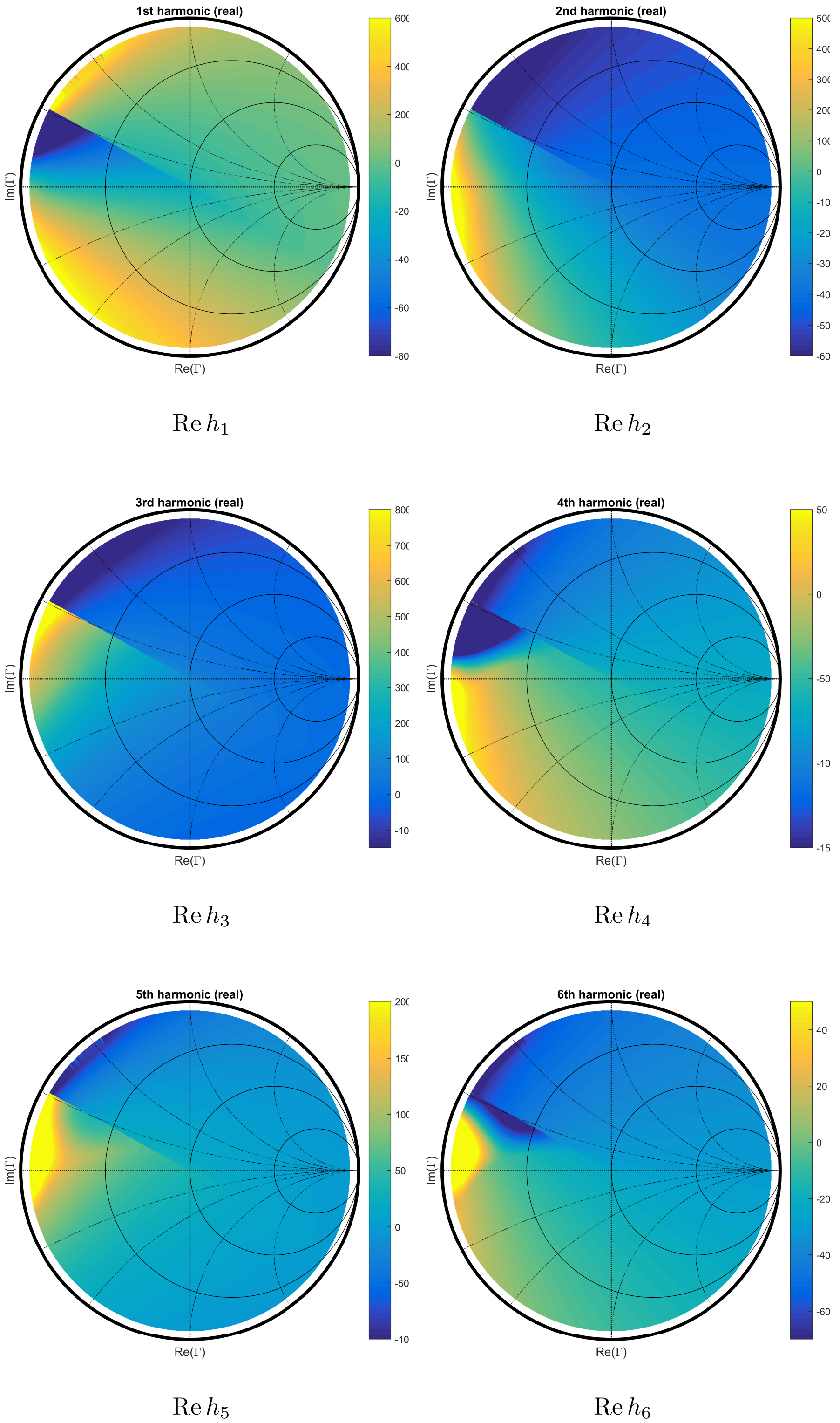

Figure D.4: Contour plot of the real part of the first six harmonics.

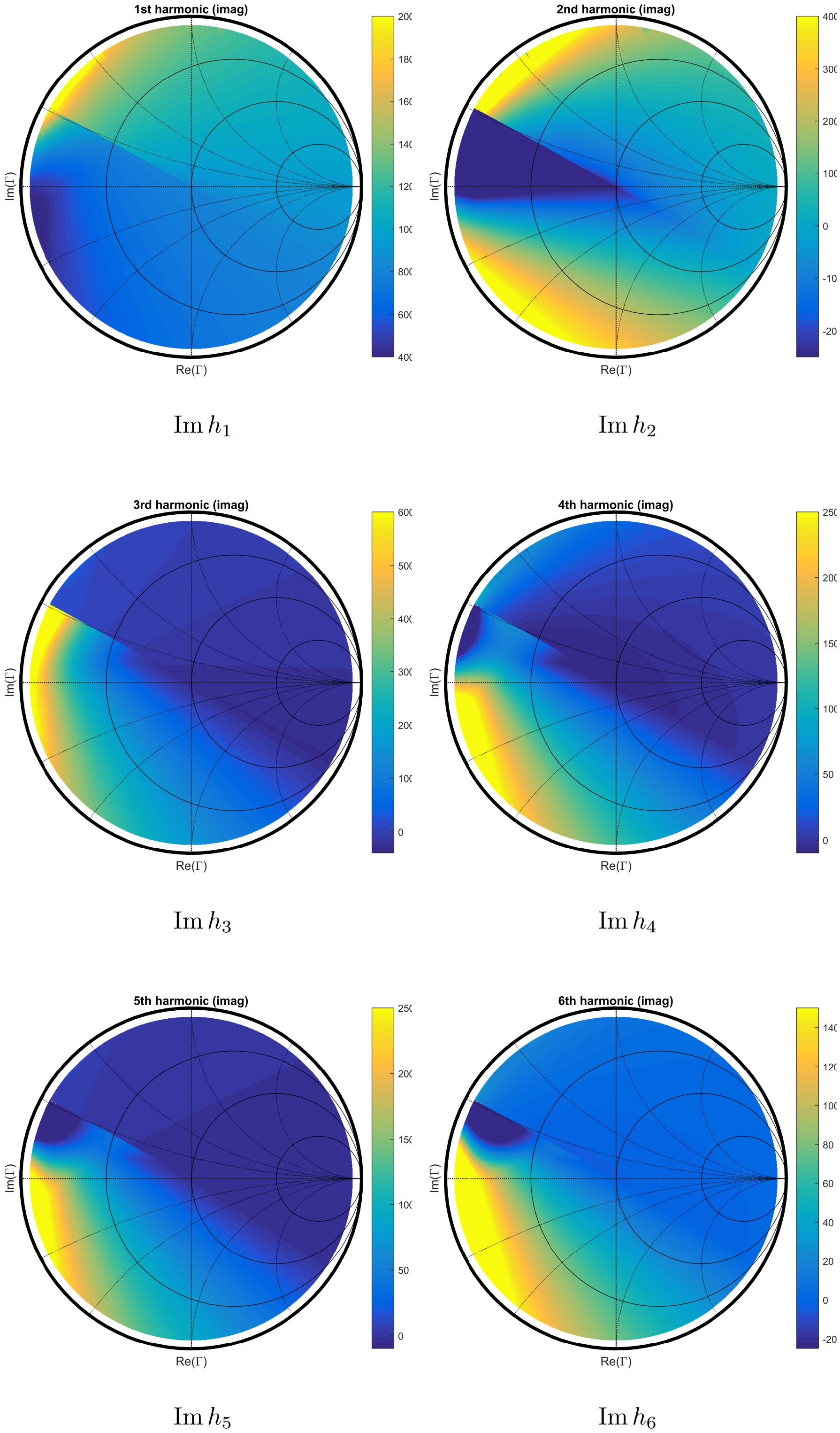

Figure D.5: Contour plot of the imaginary part of the first six harmonics.

E. Harmonic parameter gradient plots with diode

In this section the gradients of the harmonic parameters are plotted. As the distribution over the Γ_Z-plane is not as 'neat' as the simulations without the body diode effect, color plots are used instead of contour plots, and the amplitude and direction are shown in different figures.

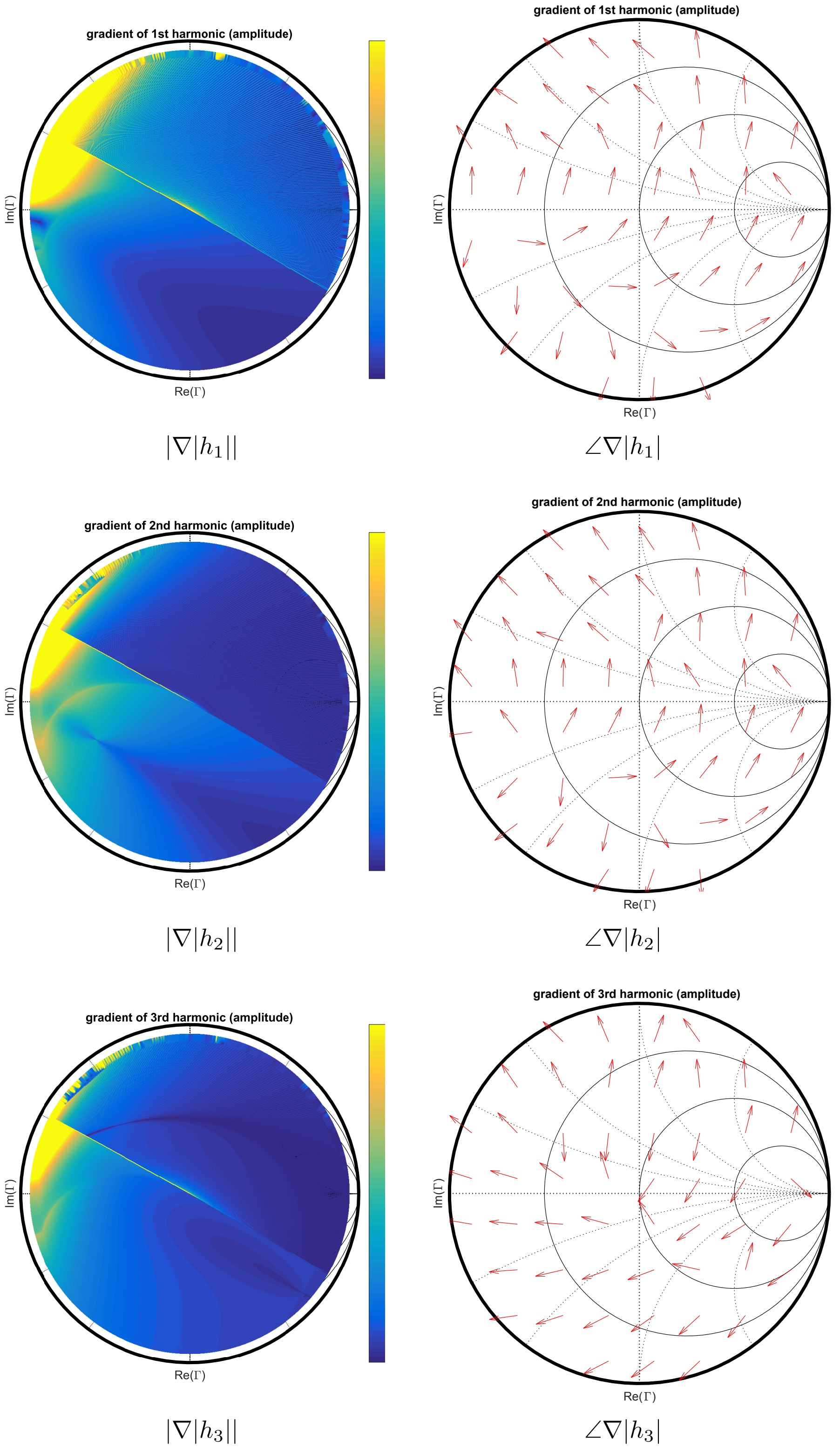

Figure E.1: Gradients of the absolute value of the first three harmonics.

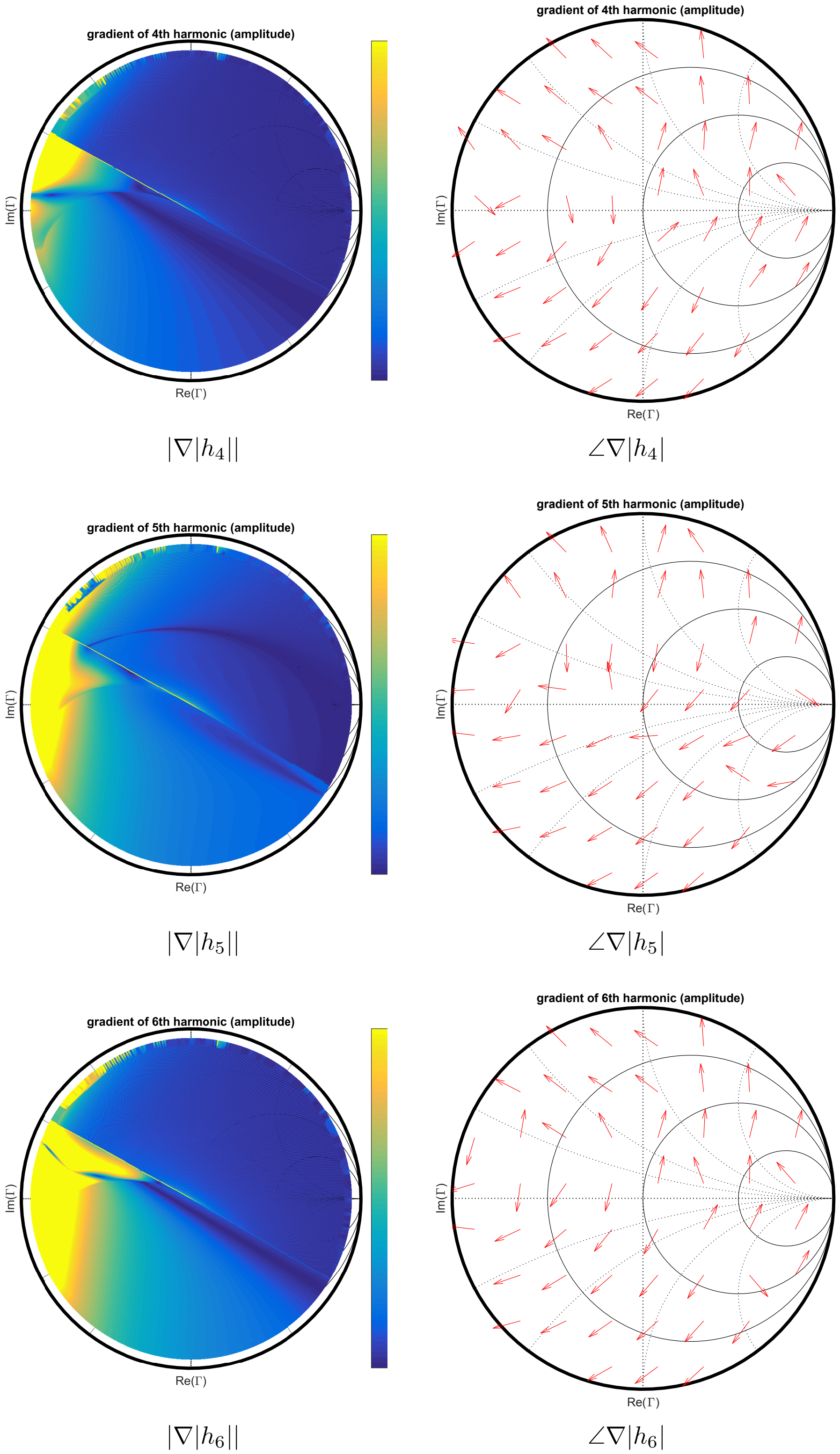

Figure E.2: Gradients of the absolute value of the harmonics four to six.

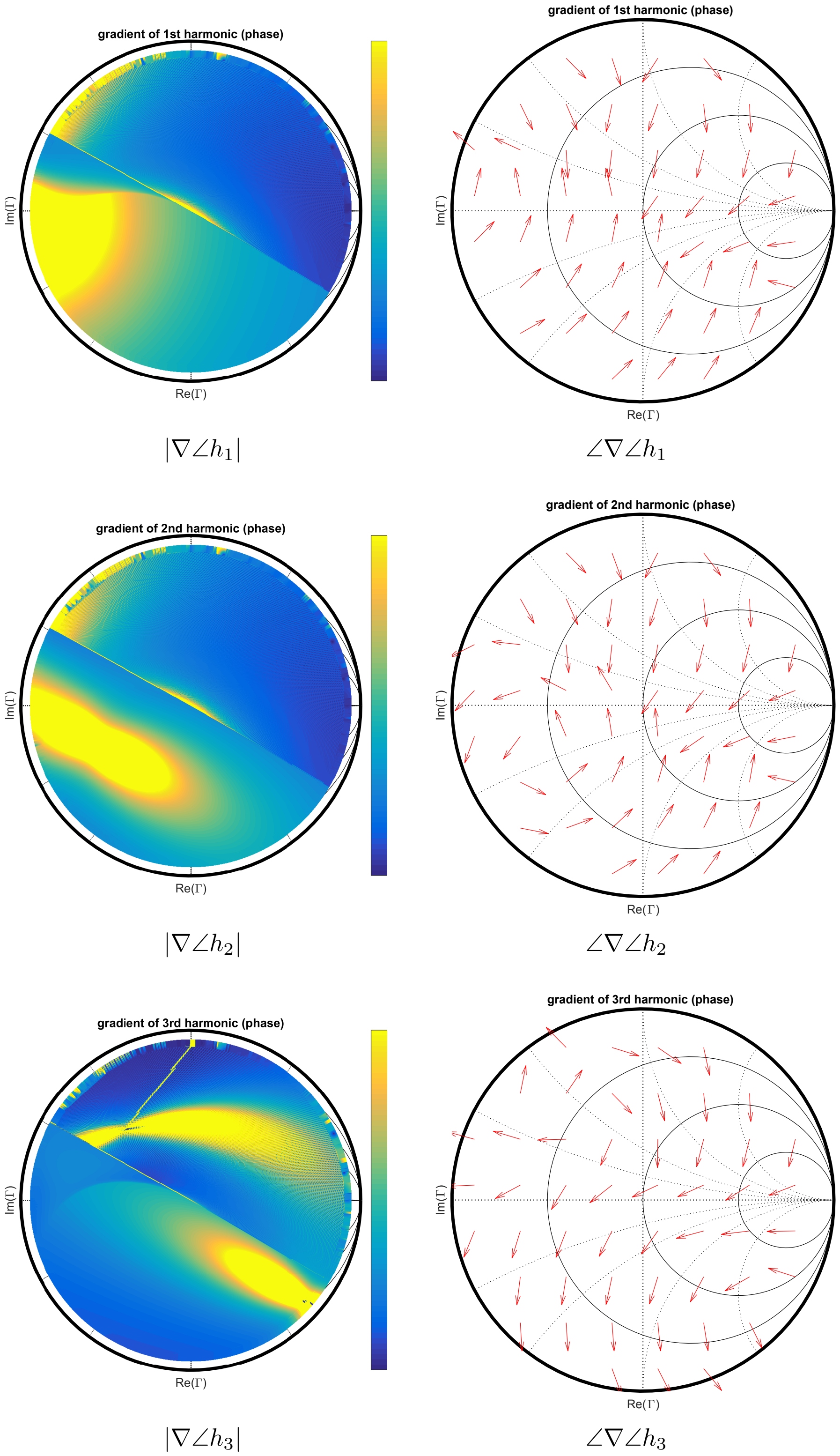

Figure E.3: Gradients of the absolute value of the first three harmonics.

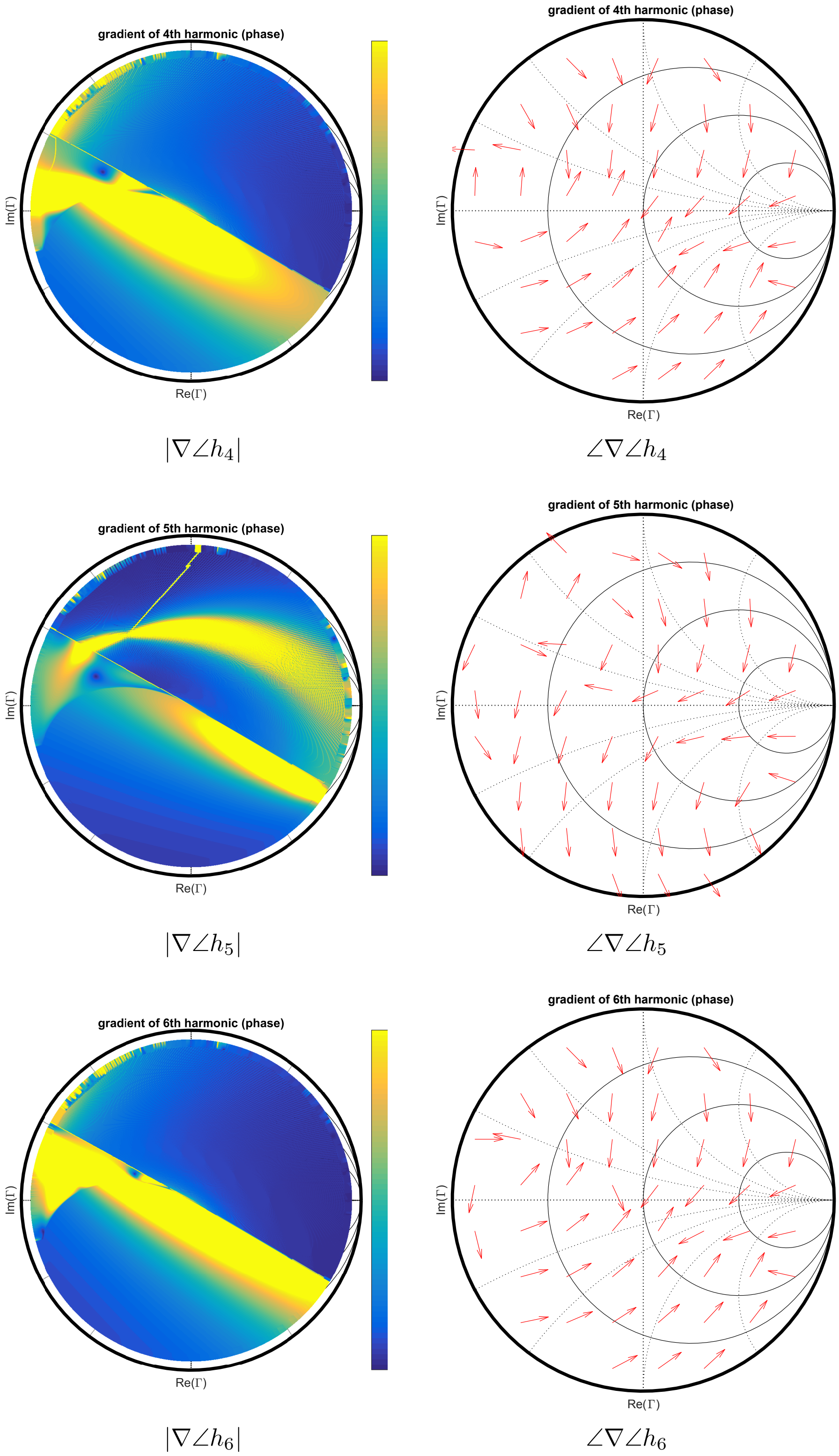

Figure E.4: Gradients of the complex phase of the harmonics four to six.

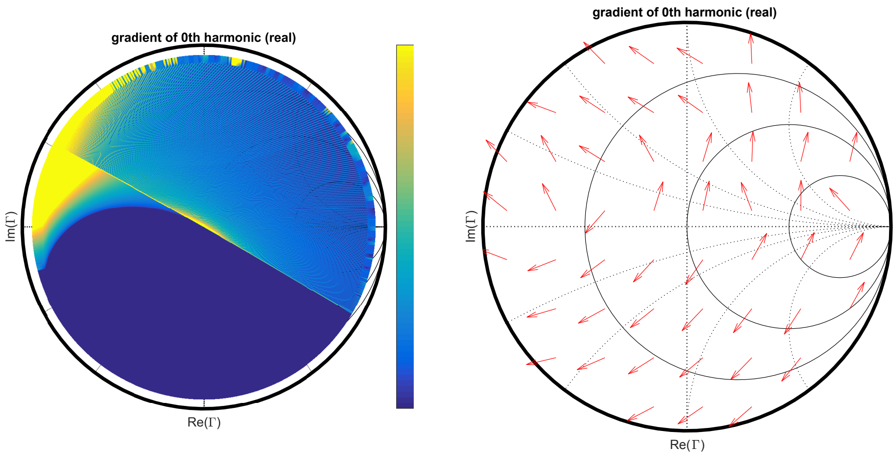

$|\nabla \operatorname{Re} h_1|$ $\angle \nabla \operatorname{Re} h_1$

Figure E.5: Gradient of the real part of the 0th harmonic (DC), $\nabla \operatorname{Re} h_0$.

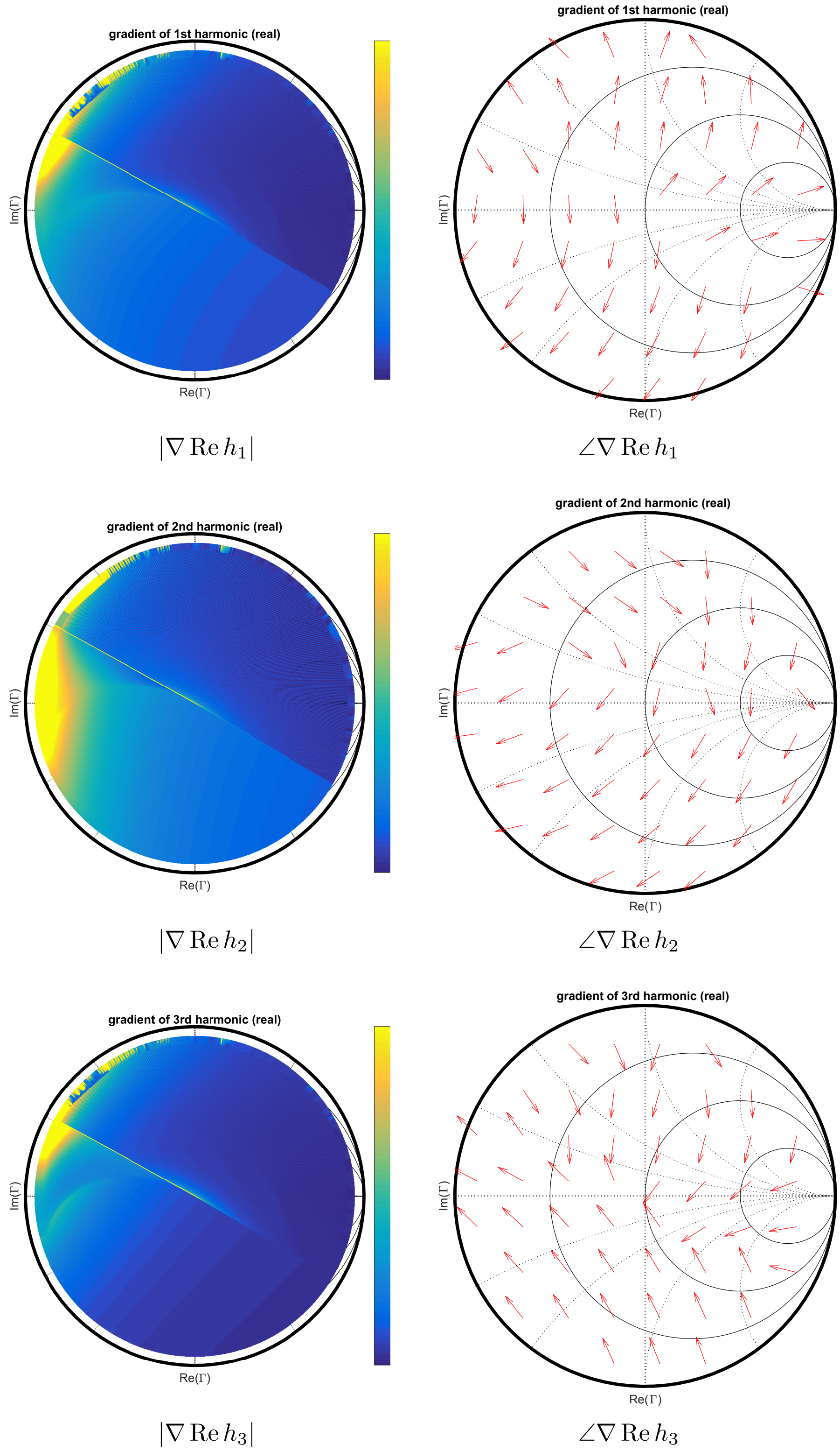

Figure E.6: Gradients of the real part of the first three harmonics.

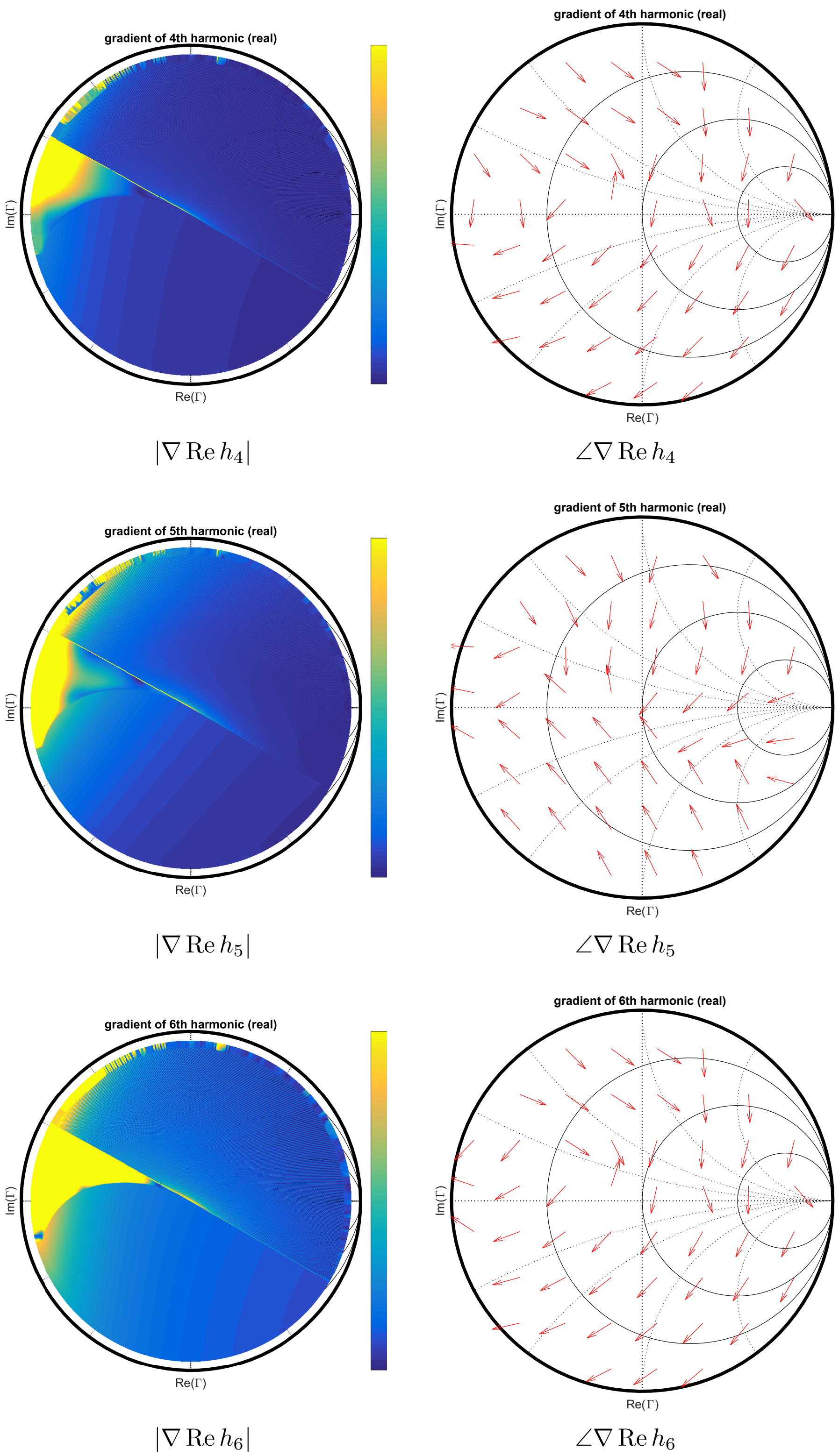

Figure E.7: Gradients of the real part of the harmonics four to six.

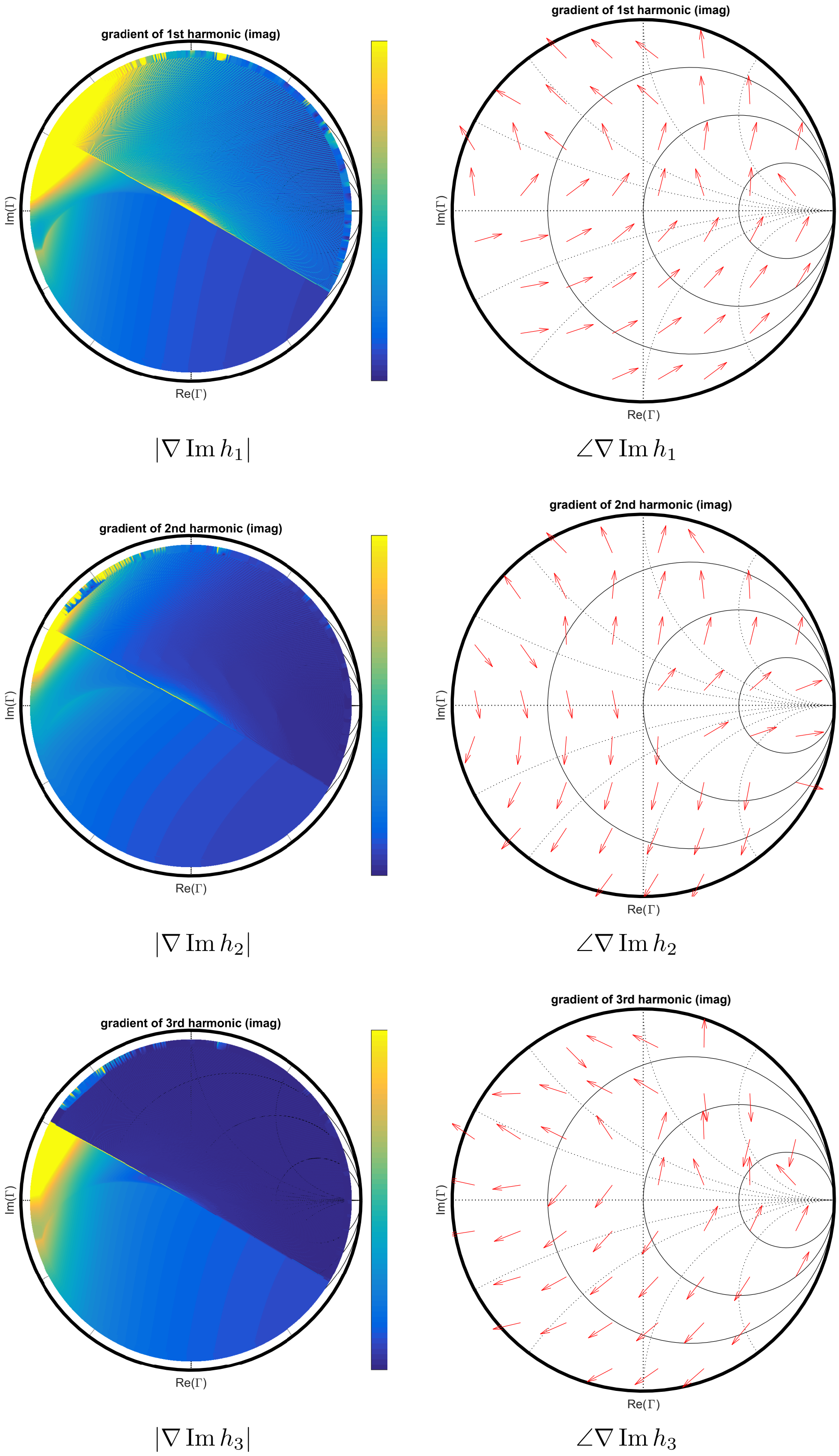

Figure E.8: Gradients of the real part of the first three harmonics.

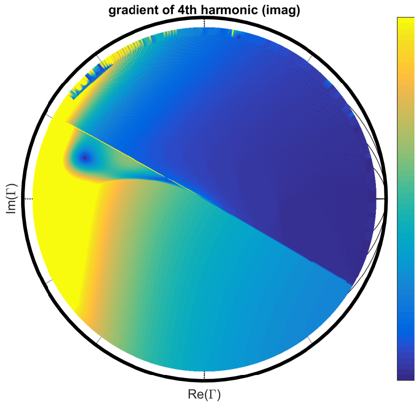

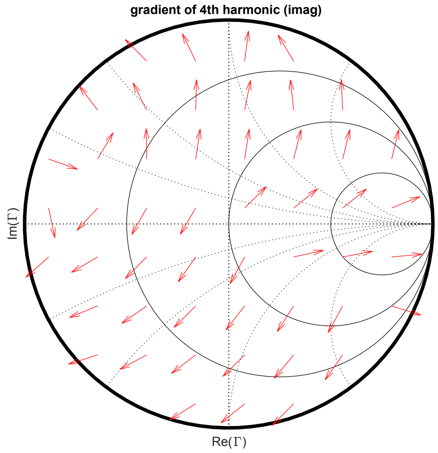

$|\nabla \operatorname{Im} h_4|$ $\angle\nabla \operatorname{Im} h_4$

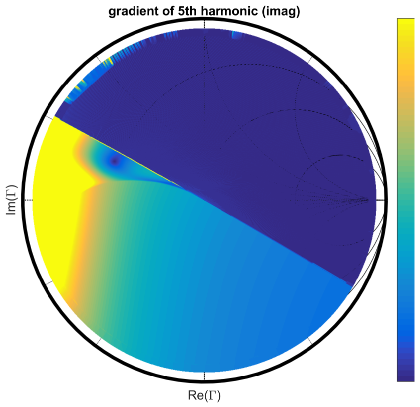

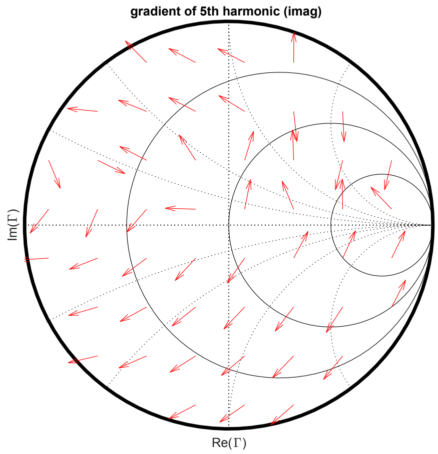

$|\nabla \operatorname{Im} h_5|$ $\angle\nabla \operatorname{Im} h_5$

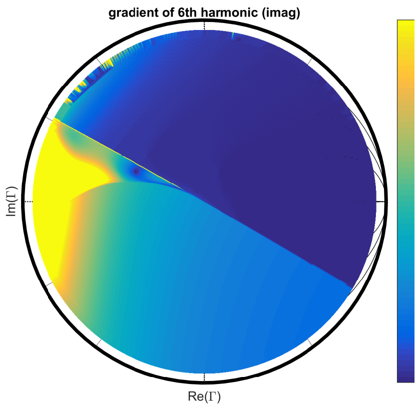

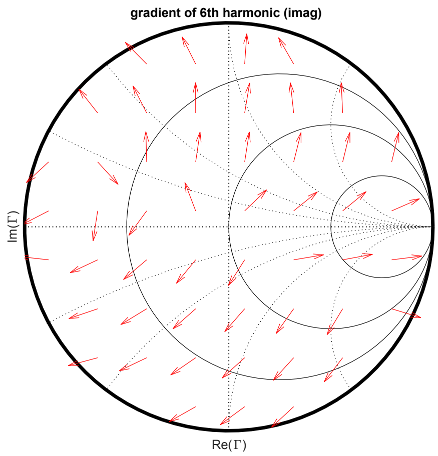

$|\nabla \operatorname{Im} h_6|$ $\angle\nabla \operatorname{Im} h_6$

Figure E.9: Gradients of the imaginary part of the harmonics four to six.

F. Harmonic parameter combinations with diode

Table F.1: Combined sensitivity value $C_{nm} \times 10^7$ for all combinations between harmonic parameters (simulated with diode) as defined in Section 6.2. The top 6 combinations that are further discussed in this section are marked in gray. A: Amplitude, P: Phase, R: Real part, I: Imaginary part.

1A	1P	1R	1I	2A	2P	2R	2I	3A	3P	3R	3I	4A	4P	4R	4I	5A	5P	5R	5I	6A	6P	6R	6I	
0.22	0.47	0.45	0.18	0.21	0.56	0.24	0.44	0.29	0.54	0.28	0.14	0.10	0.22	0.08	0.19	0.25	0.35	0.25	0.10	0.14	0.17	0.11	0.17	**0R**
-	0.78	0.60	0.22	0.41	0.94	0.50	0.64	0.61	0.78	0.53	0.41	0.19	0.31	0.15	0.31	0.42	0.45	0.40	0.20	0.25	0.23	0.20	0.27	**1A**
-	-	0.17	0.73	0.63	0.69	0.81	0.34	0.67	0.82	0.63	0.59	0.33	0.27	0.30	0.29	0.46	0.44	0.45	0.34	0.39	0.22	0.29	0.33	**1P**
-	-	-	0.64	0.48	0.62	0.78	0.20	0.56	0.71	0.48	0.56	0.29	0.28	0.26	0.27	0.41	0.37	0.39	0.30	0.37	0.22	0.30	0.30	**1R**
-	-	-	-	0.45	0.81	0.25	0.71	0.44	0.82	0.54	0.24	0.12	0.25	0.09	0.22	0.27	0.49	0.38	0.10	0.15	0.18	0.13	0.18	**1I**
-	-	-	-	-	1.07	0.60	0.49	0.53	0.74	0.49	0.42	0.25	0.30	0.20	0.29	0.40	0.41	0.38	0.26	0.30	0.23	0.22	0.28	**2A**
-	-	-	-	-	-	0.72	0.65	0.59	1.10	0.56	0.59	0.44	0.72	0.39	0.35	0.37	0.68	0.34	0.37	0.35	0.30	0.25	0.31	**2P**
-	-	-	-	-	-	-	0.87	0.44	0.69	0.60	0.16	0.21	0.19	0.17	0.20	0.18	0.47	0.32	0.11	0.08	0.13	0.07	0.12	**2R**
-	-	-	-	-	-	-	-	0.56	0.71	0.41	0.60	0.34	0.31	0.29	0.31	0.44	0.38	0.36	0.36	0.42	0.25	0.31	0.35	**2I**
-	-	-	-	-	-	-	-	-	0.73	0.24	0.22	0.26	0.24	0.22	0.23	0.16	0.46	0.21	0.21	0.24	0.18	0.18	0.21	**3A**
-	-	-	-	-	-	-	-	-	-	0.54	0.46	0.41	0.40	0.36	0.34	0.42	0.24	0.32	0.32	0.33	0.29	0.24	0.29	**3P**
-	-	-	-	-	-	-	-	-	-	-	0.38	0.32	0.27	0.26	0.29	0.27	0.33	0.09	0.29	0.30	0.20	0.20	0.27	**3R**
-	-	-	-	-	-	-	-	-	-	-	-	0.15	0.16	0.12	0.15	0.16	0.34	0.27	0.09	0.13	0.12	0.11	0.13	**3I**
-	-	-	-	-	-	-	-	-	-	-	-	-	0.13	0.04	0.09	0.20	0.24	0.25	0.07	0.12	0.10	0.11	0.12	**4A**
-	-	-	-	-	-	-	-	-	-	-	-	-	-	0.11	0.06	0.13	0.23	0.17	0.07	0.10	0.12	0.09	0.07	**4P**
-	-	-	-	-	-	-	-	-	-	-	-	-	-	-	0.11	0.17	0.21	0.22	0.04	0.11	0.09	0.10	0.10	**4R**
-	-	-	-	-	-	-	-	-	-	-	-	-	-	-	-	0.13	0.20	0.19	0.09	0.11	0.06	0.09	0.08	**4I**
-	-	-	-	-	-	-	-	-	-	-	-	-	-	-	-	-	0.30	0.12	0.12	0.10	0.09	0.09	0.09	**5A**
-	-	-	-	-	-	-	-	-	-	-	-	-	-	-	-	-	-	0.22	0.19	0.21	0.17	0.16	0.17	**5P**
-	-	-	-	-	-	-	-	-	-	-	-	-	-	-	-	-	-	-	0.20	0.17	0.12	0.10	0.17	**5R**
-	-	-	-	-	-	-	-	-	-	-	-	-	-	-	-	-	-	-	-	0.07	0.06	0.07	0.06	**5A**
-	-	-	-	-	-	-	-	-	-	-	-	-	-	-	-	-	-	-	-	-	0.06	0.04	0.03	**6A**
-	-	-	-	-	-	-	-	-	-	-	-	-	-	-	-	-	-	-	-	-	-	0.05	0.04	**6P**
-	-	-	-	-	-	-	-	-	-	-	-	-	-	-	-	-	-	-	-	-	-	-	0.06	**6R**